Princetonlaan 6
3584 CB Utrecht
P.O. Box 80015
3508 TA Utrecht
The Netherlands

www.tno.nl

T +31 88 866 42 56

TNO report

VELMOD-3.2

Date	21 March 2024
Author(s)	B.F. Paap, J.C. Doornenbal, M. den Dulk, J.M.M. Hettelaar
Number of pages	62 (incl. appendices)
Number of appendices	3
Project name	GIP 2023 - Kartering Diepe Ondergrond
Project number	060.55743

Contents

1 Introduction

VELMOD-3.2 is the Dutch national velocity model of the subsurface and successor of VELMOD-3.1 (Pluymaekers et al., 2017). Similar to VELMOD-3.1, VELMOD-3.2 is based on velocity data from sonic logs and checkshot data to which depth markers of lithostratigraphic layer boundaries have been assigned. With this data a *layer-cake* velocity model is constructed based on V_0-k parameterization. The approach used for developing VELMOD-3.2 corresponds to VELMOD-3.1, but it consists of two main improvements:

1) The use of refined selection criteria of velocity data based on Doornenbal et al. (2021). This approach was developed within the GeoERA research project 3DGEO-EU where a harmonized cross-border velocity model was developed for the Northern cross-border part of the North Sea.
2) The use of recent depth information of tops of main stratigraphic units based on a database extraction from DINO (dinoloket.nl, December 2021)

The primary application of the VELMOD-3.2 model is time to depth conversion for large scale (regional) seismic interpretation and mapping in the Netherlands.

2 Data

2.1 Velocity data

The used velocity dataset consists of sonic logs and checkshot data. Sonic data from different logging tools were available, often expressed in different formats like slowness, instantaneous sonic velocity and (calibrated) traveltime-depth (TZ) pairs. The dataset comprises digital available well data released to the public domain before November 1st 2021. All borehole data files used within this project are listed in appendix A.

2.2 Deviation data

All used deviation data were available from DINO (the National Geo-data Centre of the Netherlands), through the 'NL Olie- en Gasportaal' at www.nlog.nl.

2.3 Lithostratigraphic marker data

Borehole lithostratigraphic marker data were retrieved from DINO. These markers are assigned conform the standard stratigraphic nomenclature of the Netherlands (Van Adrichem Boogaert & Kouwe, 1993-1997). The lithostratigraphic data was aggregated from stratigraphic member level to main stratigraphic (sub) group level (Figure 3.1).

2.4 Data processing

The major part of the data processing workflow used for VELMOD-3.2 corresponds to VELMOD-3.1, and the workflow is depicted in Figure 2.1. All raw velocity data was subject to quality control in terms of (velocity) data type and accompanying data unit. Per well the dataset was checked on completeness. Wells without stratigraphic information were discarded. Wells without deviation data were considered to be vertical. The aggregated stratigraphic data was QC-ed on completeness and updated when necessary.

All velocity datasets were normalized to TVDSS (m), time (s), velocity (m/s). Duplicate depth/time values were removed. Datasets with depth and/or time reversals (mainly checkshot data) were discarded from analysis. All normalized velocity data was stored in a database together with metadata, deviation data and stratigraphic data from the wells.

For VELMOD-3.2 the following improvements in data-selection and processing were made compared to VELMOD-3.1:

- A more recent interpretation of depths of well tops from main stratigraphic units was incorporated (from December 2021). This also resulted in additional velocity information for certain stratigraphic units that was not included in VELMOD-3.1.
- Problematic wells as contained in the list of well rejections were not included in the analysis (see appendix A).
- VELMOD-3.1 contained an error when calculating lateral midpoints (x and y coordinates) of stratigraphic units along the well trajectory. These midpoints were used to create V_0 and V_{int} grids, in turn introducing a bias in resulting grids in the vicinity of the used wells. This error has been resolved in VELMOD-3.2.

- An error existing in VELMOD-3.1 was resolved concerning the incorrect assignment of mid-depths and interval velocity to the North Sea Supergroup (N) , in case the Upper North Sea Group (NU) was not present.
- Only velocity data was used that covered more than 90% of the stratigraphic intervals, since this provides more reliable data.
- Only velocity data was used where a minimum of 5 ms of a stratigraphic interval was recorded.
- For constructing final grids of V_0 and V_{int}, velocity data from the offshore parts of the United Kingdom, Germany and Denmark were used for more accurate data interpolation along the borders of the Dutch area. However, foreign data could not be used for gridding of the Upper North Sea Group, the Holland formation and the Vlieland Subgroup due to a lack of data. Also note that the foreign velocity data was not used for the model parameterization (V_{int}-Z_{mid} analysis, see section 3.3-3.5)

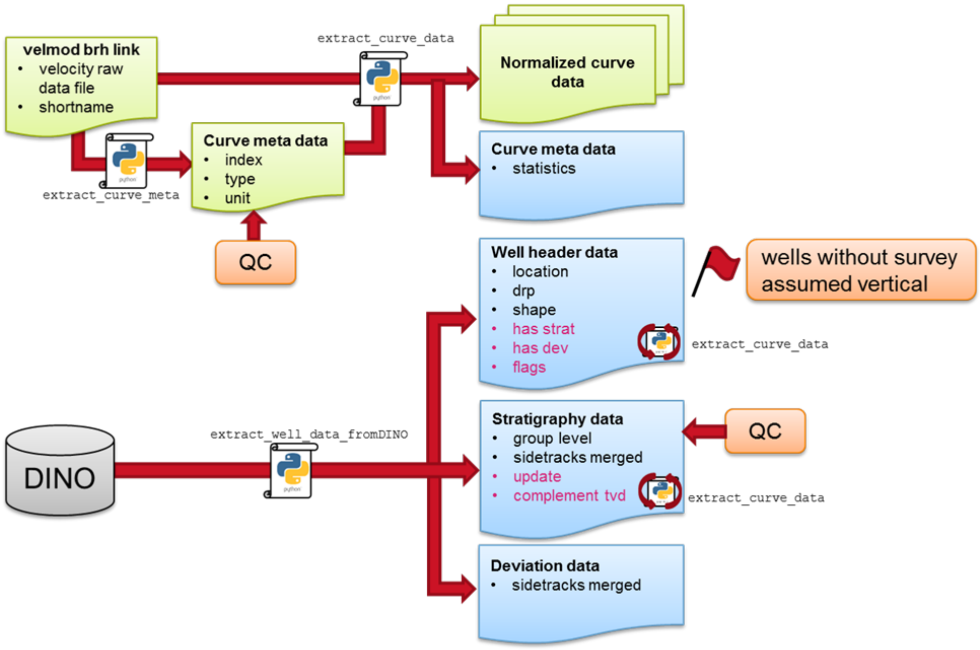

Figure 2.1 Overview of data processing workflow.

3 VELMOD velocity models

3.1 Layer cake model

Within this project a ‘layer cake’ type velocity model is used. For each defined stratigraphic layer (Figure 3.1) seismic velocity is modelled. Nine main stratigraphic units are distinguished.

- Three layers (1, 3 and 6) were split into two sublayers and modelled individually.
- Only the Zechstein Group (layer 7 in Figure 3.1) was modelled with a different method (see chapter 3.4).
- For the Limburg Group also the Geul Subgroup (DCG) was modelled individually.

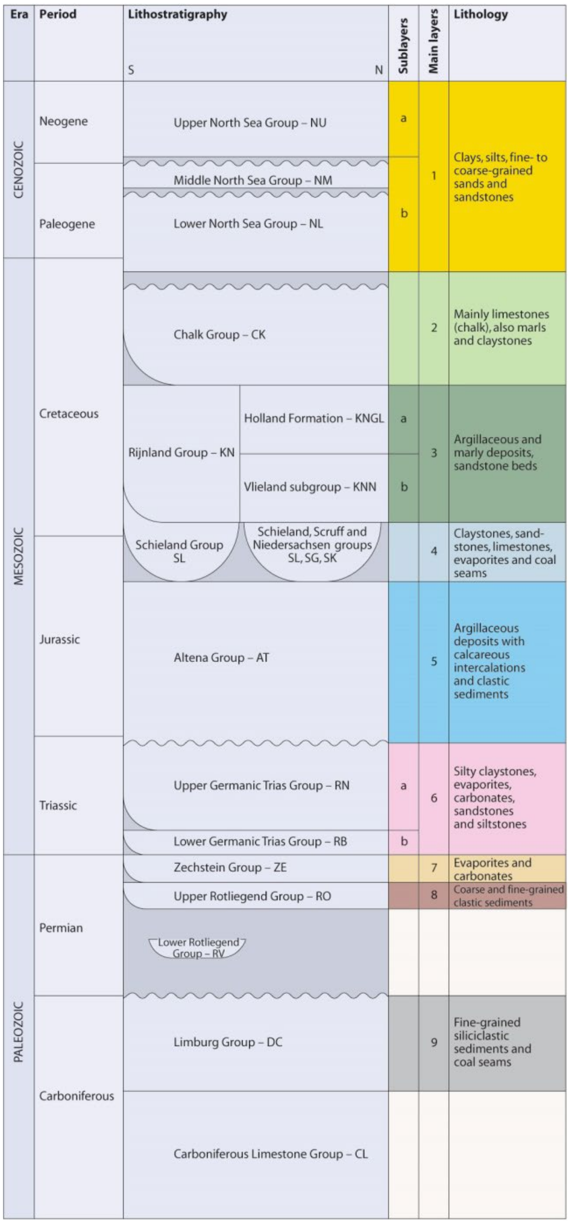

Figure 3.1 Layer cake model of VELMOD-3 based on lithostratigraphy after Van Adrichem Boogaert and Kouwe (1993-1997).

3.2 Compacting layers

Except the layer of the Zechstein Group (Figure 3.1, layer 7), all layers have been subjected to considerable compaction due to sediment loading during burial phases. This compaction resulted in an increase of compressional wave velocity of layer sediments with burial depth.
For the compacting layers, we adopt model velocities that increase linearly with depth. A velocity model of this type is completely described by:

$$V = V_0 + k\,Z \qquad \text{(eq. 1)}$$

Where V [m/s] is the instantaneous velocity, V_0 [m/s] the normalized velocity, k [m/s/m] the velocity-depth gradient and Z [m] the depth.

3.3 General model parameterization

The V_0 and k model parameters were determined according to the V_{int} - Z_{mid} method applied per stratigraphic layer. This method approximates the regional velocity-depth gradient, as well as a regional normalized velocity. In Figure 3.1 all interval velocity values (V_{int}) for all lithostratigraphic groups except Zechstein Group have been plotted against the mid depth (Z_{mid}). From this figure could be clearly concluded that there is a general increase of velocity with depth but also that the values per interval could be grouped or characterised by a certain dip (k value) and a certain V_0 value: see for example the clear differences in the North Sea Supergroup values (yellow), Chalk Group (light green), Rijnland Group (dark green) and most of the other groups.

Table 3.1 and Figure 3.3 to Figure 3.16 show the results of the V_0 and k parameterization. Note that for the Upper-Jurassic Supergroup a further distinction into 3 basins clusters for different structural elements was made (see Table 3.1), like Pluymaekers et al. (2017).

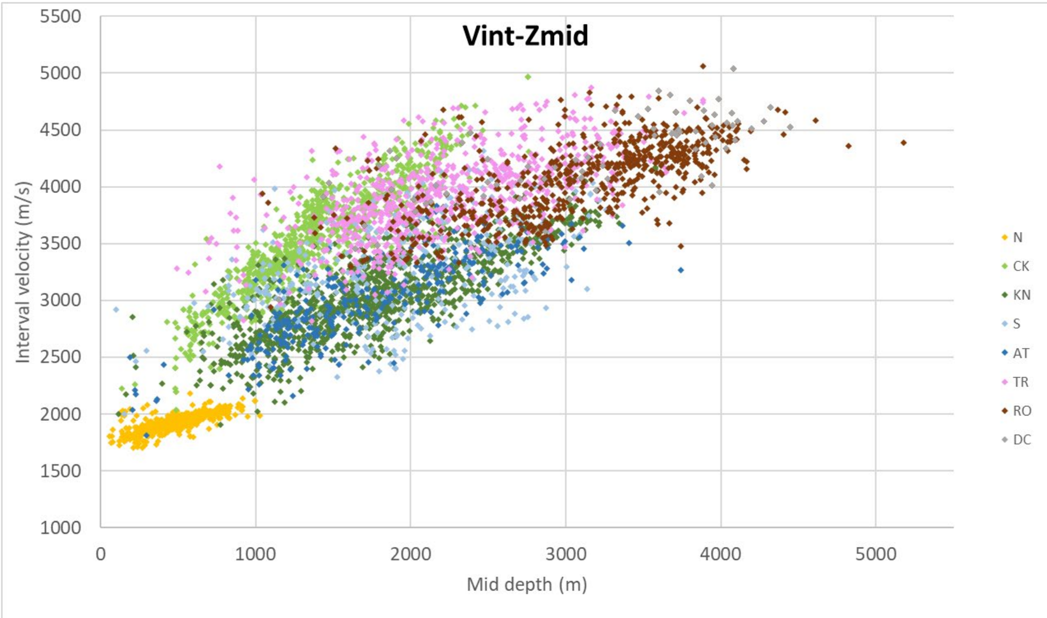

Figure 3.1 Interval velocity vs mid depth for each main lithostratigraphic group. See Figure 3.1 for the meaning of the abbreviations.

Velocity curves covering less than 90% of the drilled stratigraphic interval were discarded from the regression analysis. Also, velocity curves with an interval velocity lower than 1600 m/s and higher than 6500 m/s were discarded from analysis. If the remaining dataset contained multiple velocity curves for a single well, the velocity curve with the smallest deviation with respect to the global V_{int} - Z_{mid} regression line was marked as the preferred velocity curve. The global regression line is based on a linear least-square regression of V_{int} on Z_{mid}.

Table 3.1 V_{int} - Z_{mid} regression data for the main layers of VELMOD-3.2. Here r represents the correlation coefficient. The meaning of the stratigraphic abbreviations used, can be found in Figure 3.1.

Layer	Stratigraphic unit	Area	Number of Boreholes	k (s-1)	V_0-global (m/s)	r
1	N	Dutch territory	540	0.31	1782	0.69
1a	NU	Dutch territory	404	0.44	1761	0.67
1b	NM+NL	Dutch territory	687	0.21	1797	0.54
2	CK	Dutch territory	987	0.93	2253	0.90
3	KN	Dutch territory	1115	0.50	2142	0.82
3a	KNGL	Dutch territory	1062	0.66	1951	0.90
3b	KNN	Dutch territory	974	0.43	2190	0.68
4	S_all	Dutch territory	382	0.26	2787	0.39
4	S1	Lower Saxony Basin, Central Netherlands Basin, West Netherlands Basin, Broad Fourteens Basin	233	0.52	2513	0.66
4	S2	Vlieland Basin, Terschelling Basin, Step Graben	48	0.77	1445	0.81
4	S3	Dutch Central Graben	69	0.66	1426	0.71
5	AT	Dutch territory	344	0.45	2210	0.78
6	RN+RB	Dutch territory	898	0.38	3034	0.64
6a	RN	Dutch territory	566	0.38	3108	0.65
6b	RB	Dutch territory	809	0.40	3072	0.65
8	RO	Dutch territory	721	0.33	3040	0.66
9	DC	Dutch territory	435	0.26	3444	0.65
9	DCG	Dutch territory	15	0.36	3179	0.91

N

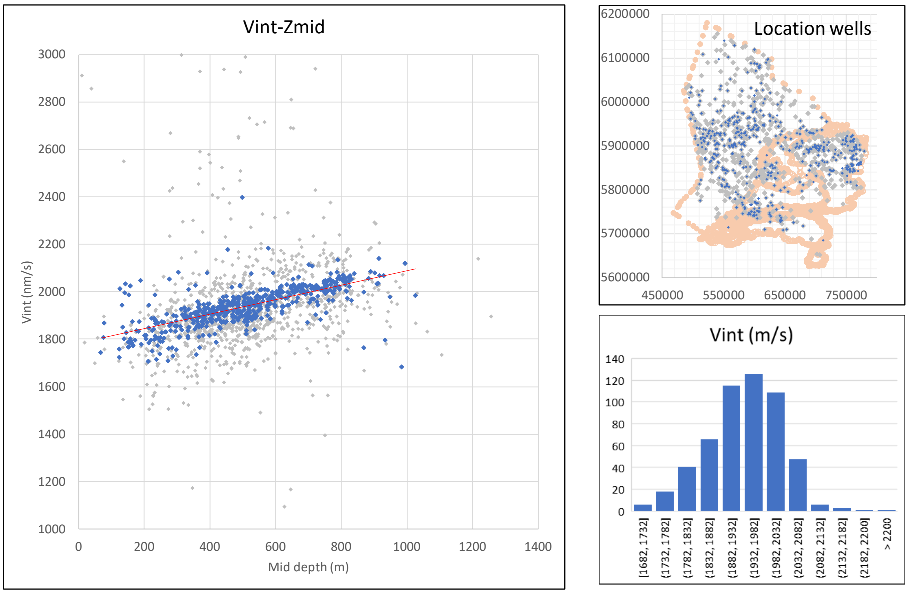

Figure 3.2 Interval velocity vs mid-depth (left), distribution (lower right) and location (upper right) of interval velocities of the North Sea Supergroup. Note 1: the grey points in the plot of interval velocity vs mid-depth (left) are discarded from regression analysis, because of the data processing and selection procedure described in sections 2 and 3. Note 2: the lower right plot of the distribution shows the number of occurrence (vertical axis) of different bins of the interval velocity (horizontal axis). This applies to Figure 3.2 up to Figure 3.16

NU

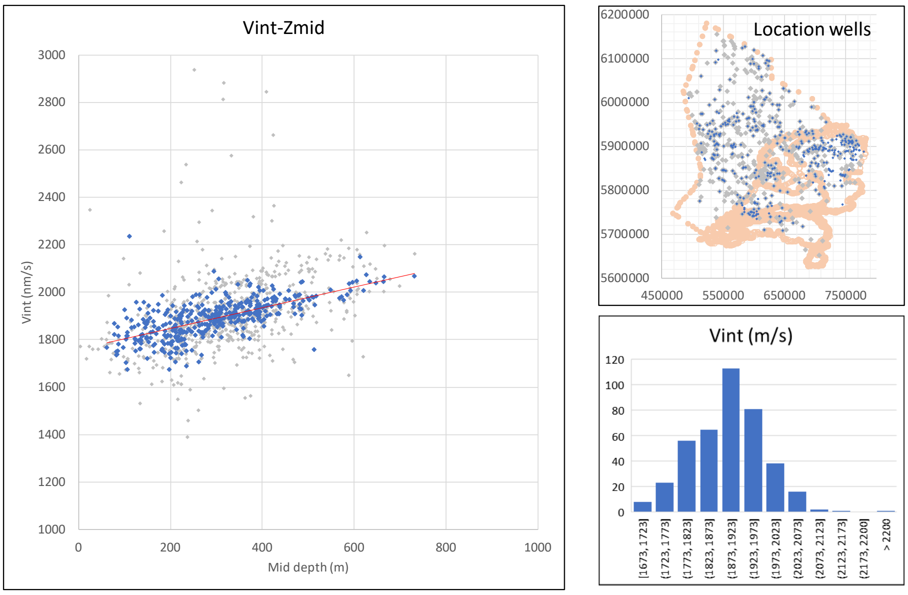

Figure 3.3 Interval velocity vs mid-depth (left; grey points are discarded from regression analysis), distribution (lower right) and location (upper right) of interval velocities of the Upper North Sea Group

NLM

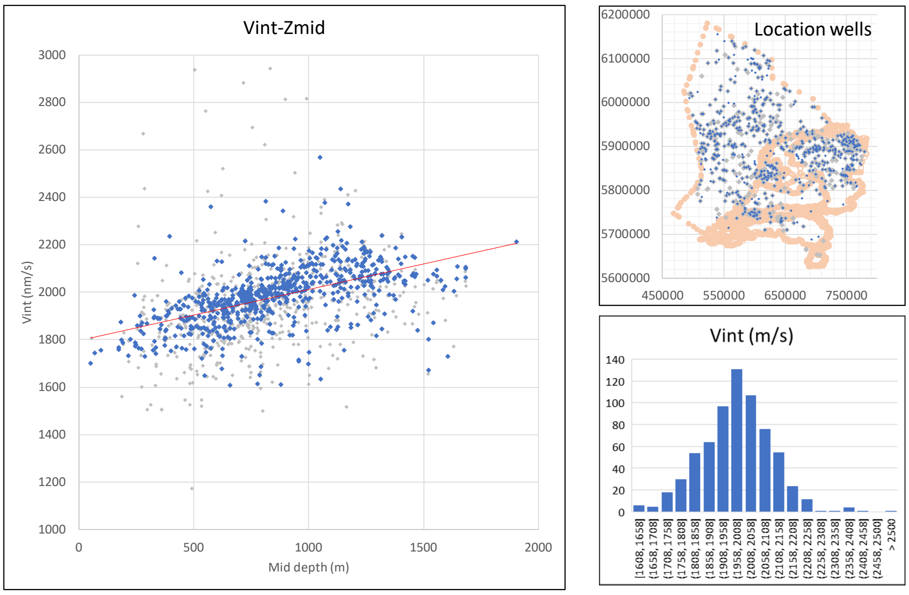

Figure 3.4 Interval velocity vs mid-depth (left; grey points are discarded from regression analysis), distribution (lower right) and location (upper right) of interval velocities of the Middle and Lower North Sea groups.

CK

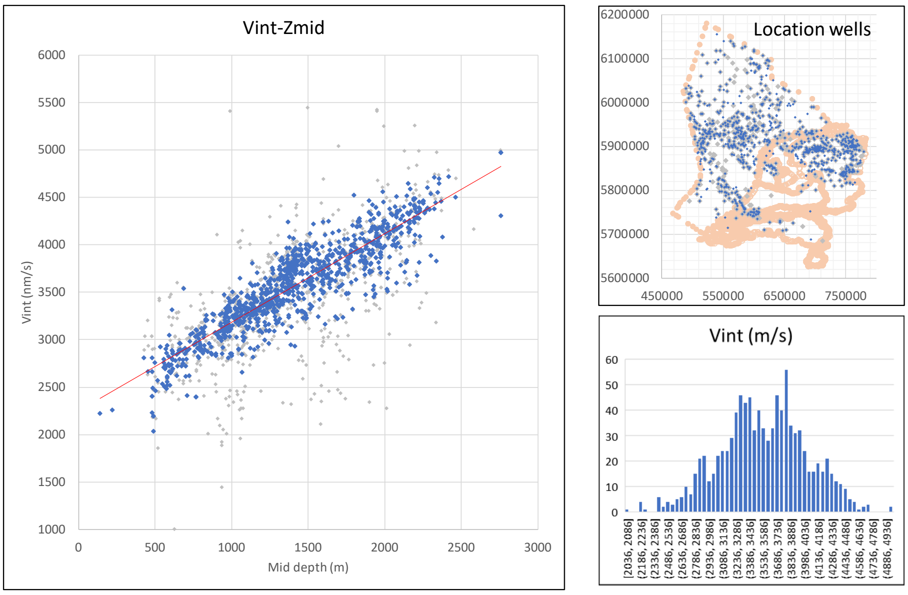

Figure 3.5 Interval velocity vs mid-depth (left; grey points are discarded from regression analysis), distribution (lower right) and location (upper right) of interval velocities of the Chalk Group.

KN

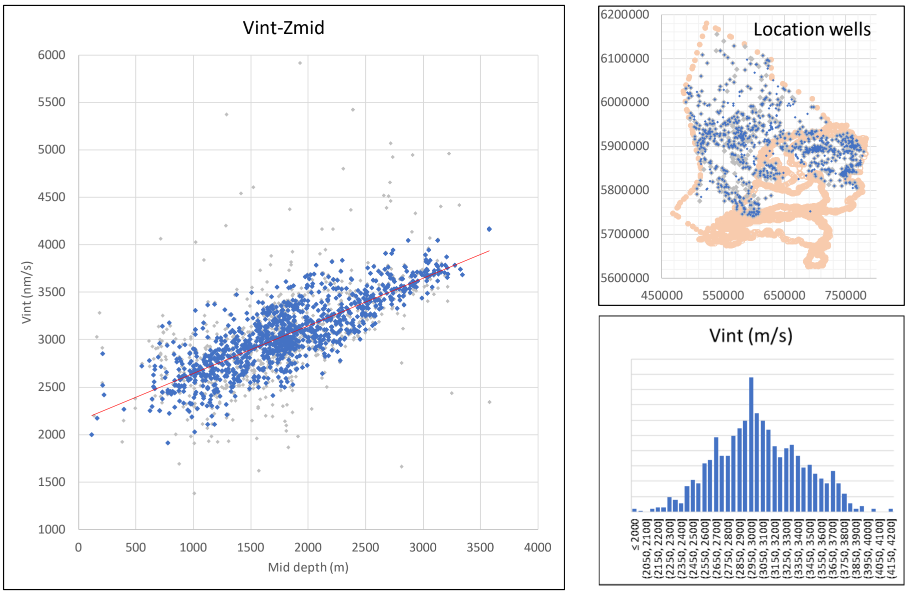

Figure 3.6 Interval velocity vs mid-depth (left; grey points are discarded from regression analysis), distribution (lower right) and location (upper right) of interval velocities of the Rijnland Group.

KNG

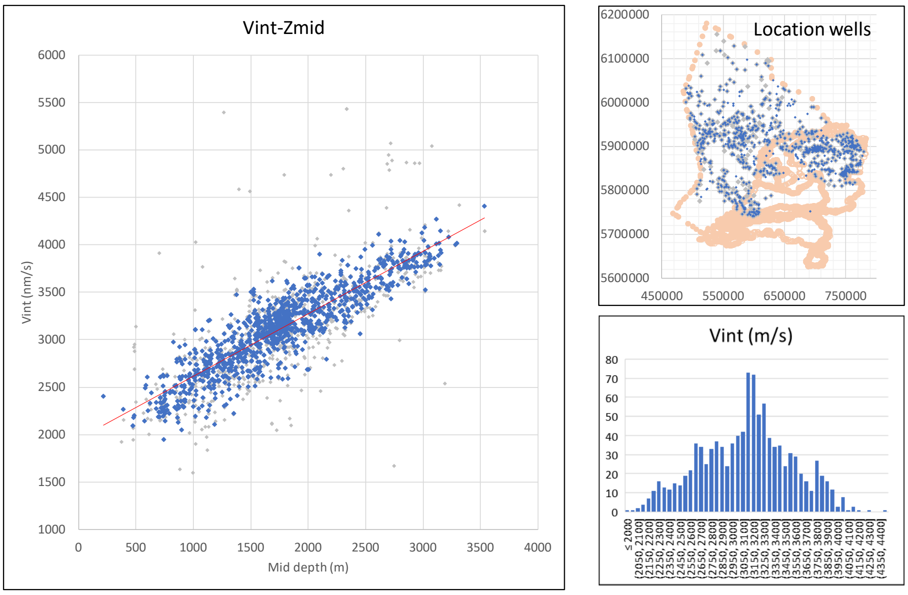

Figure 3.7 Interval velocity vs mid-depth (left; grey points are discarded from regression analysis), distribution (lower right) and location (upper right) of interval velocities of the Holland Formation (upper part of Rijnland Group).

KNN

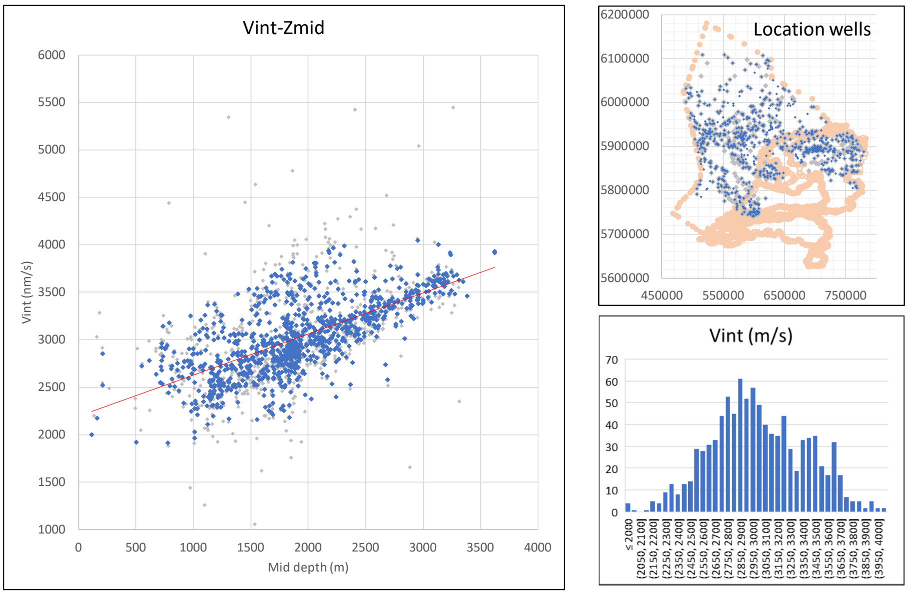

Figure 3.8 Interval velocity vs mid-depth (left; grey points are discarded from regression analysis), distribution (lower right) and location (upper right) of interval velocities of the Vlieland Subgroup (lower part of Rijnland Group).

S

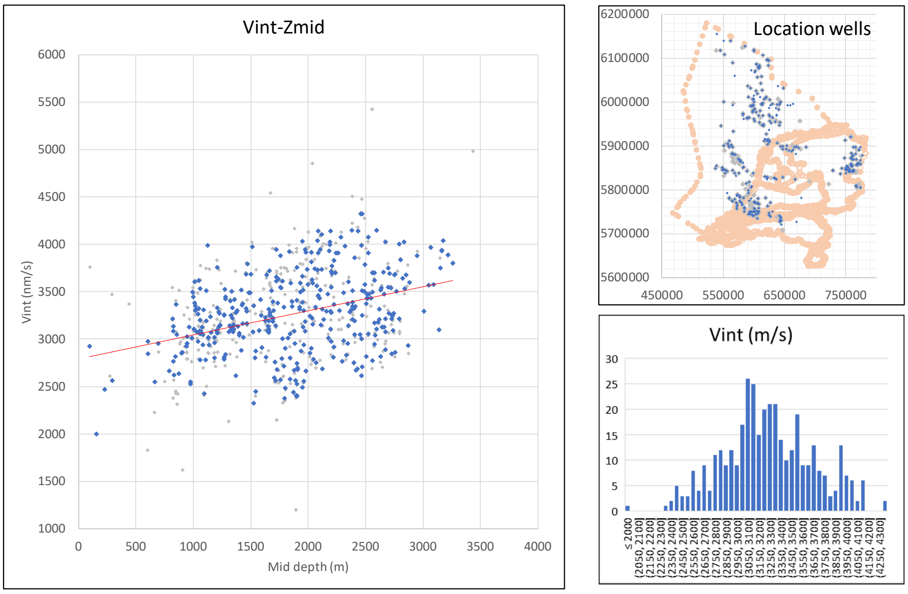

Figure 3.9 Interval velocity vs mid-depth (left; grey points are discarded from regression analysis), distribution (lower right) and location (upper right) of interval velocities of the Upper-Jurassic Supergroup.

AT

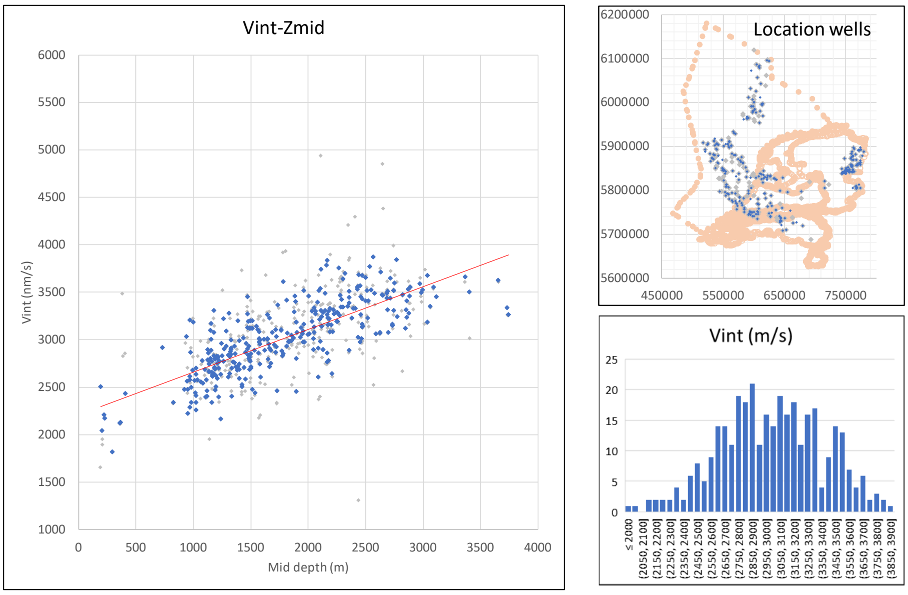

Figure 3.10 Interval velocity vs mid-depth (left; grey points are discarded from regression analysis), distribution (lower right) and location (upper right) of interval velocities of the Altena Group.

RN+RB

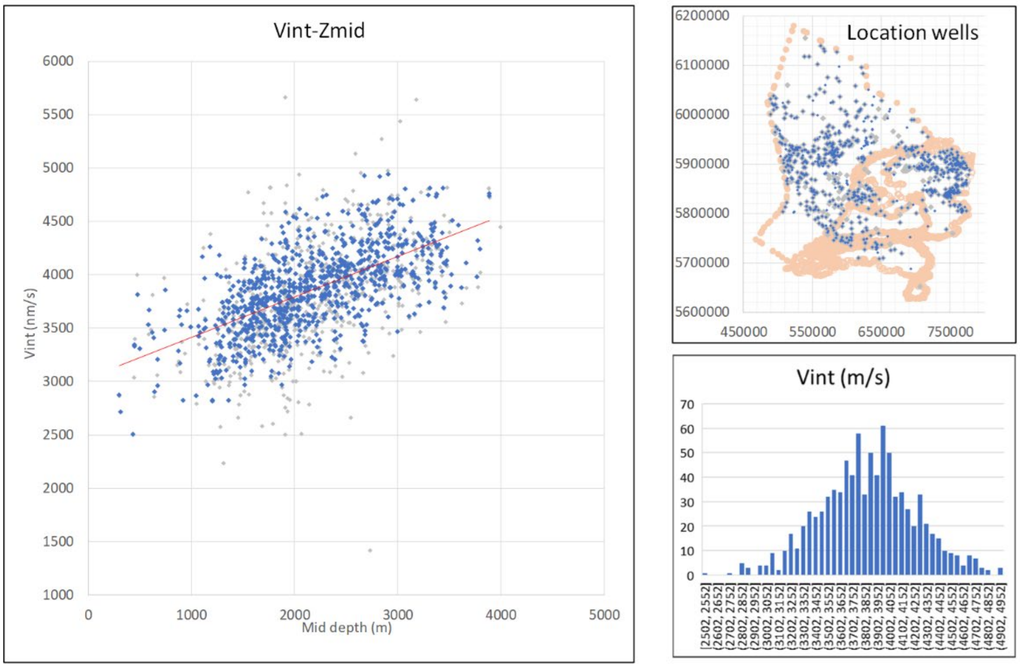

Figure 3.11 Interval velocity vs mid-depth (left; grey points are discarded from regression analysis), distribution (lower right) and location (upper right) of interval velocities of the Upper and Lower Germanic Trias groups.

RN

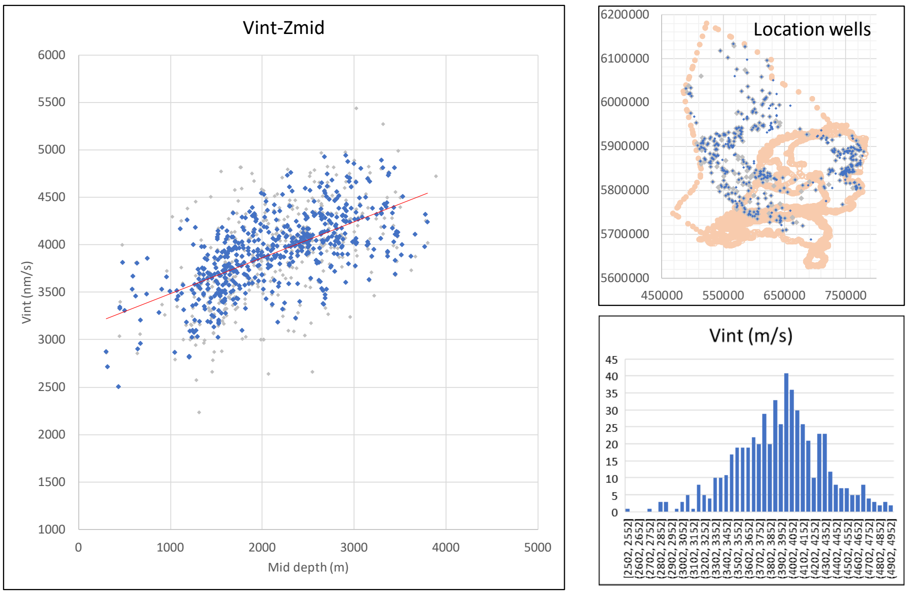

Figure 3.12 Interval velocity vs mid-depth (left; grey points are discarded from regression analysis), distribution (lower right) and location (upper right) of interval velocities of the Upper Germanic Trias Group.

RB

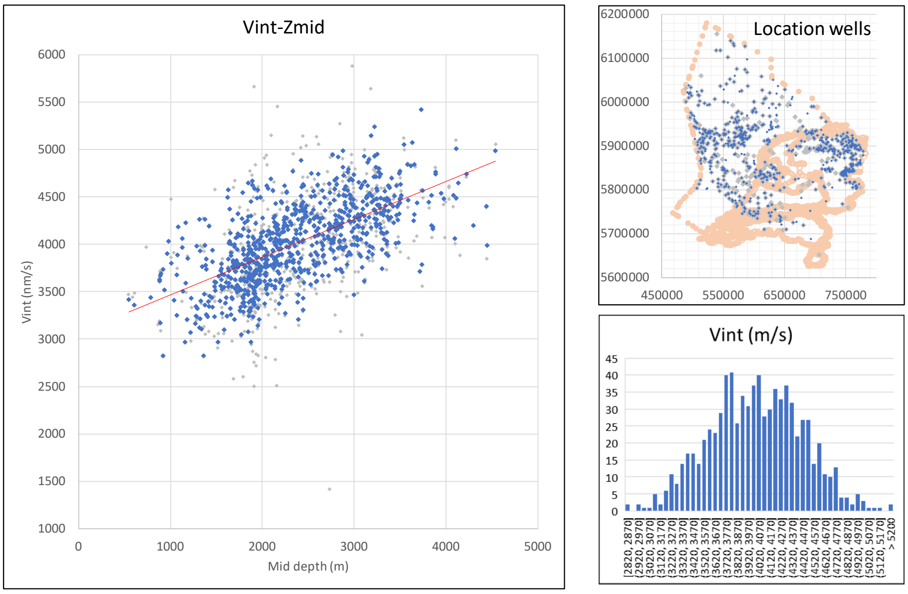

Figure 3.13 Interval velocity vs mid-depth (left; grey points are discarded from regression analysis), distribution (lower right) and location (upper right) of interval velocities of the Lower Germanic Trias Group.

RO

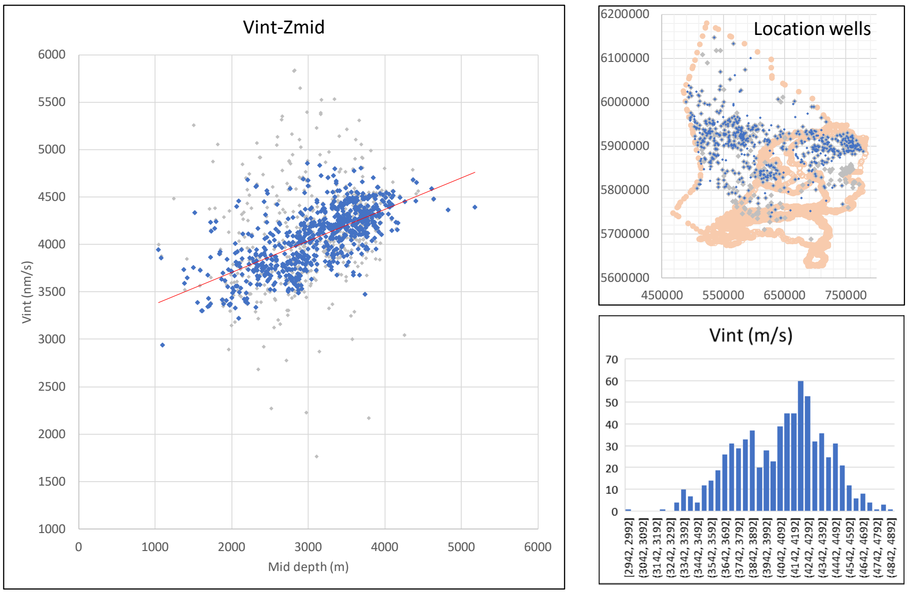

Figure 3.14 Interval velocity vs mid-depth (left; grey points are discarded from regression analysis), distribution (lower right) and location (upper right) of interval velocities of the Upper Rotliegend Group.

DC

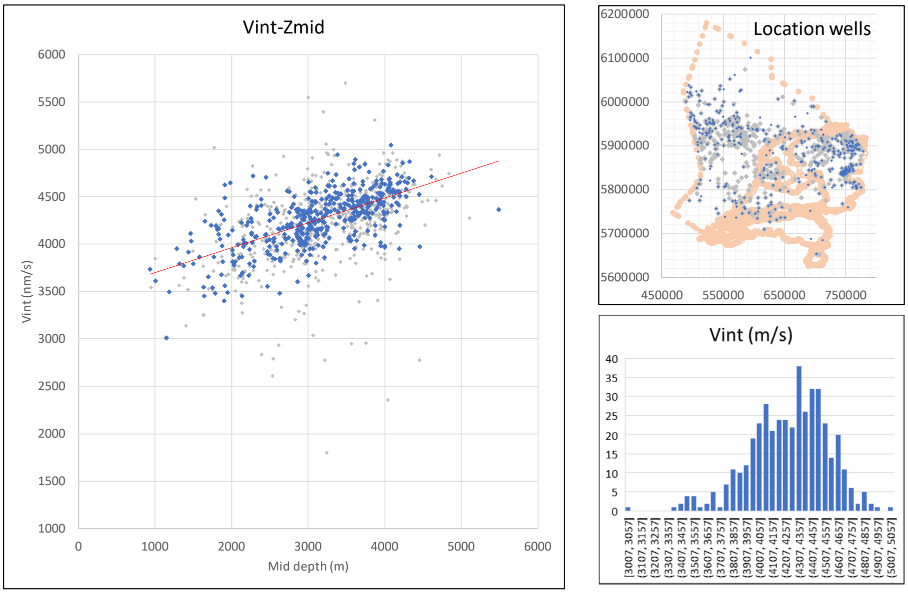

Figure 3.15 Interval velocity vs mid-depth (left; grey points are discarded from regression analysis), distribution (lower right) and location (upper right) of interval velocities of the Limburg Group, the vast majority only penetrates the upper part of Westphalian aged strata.

DCG

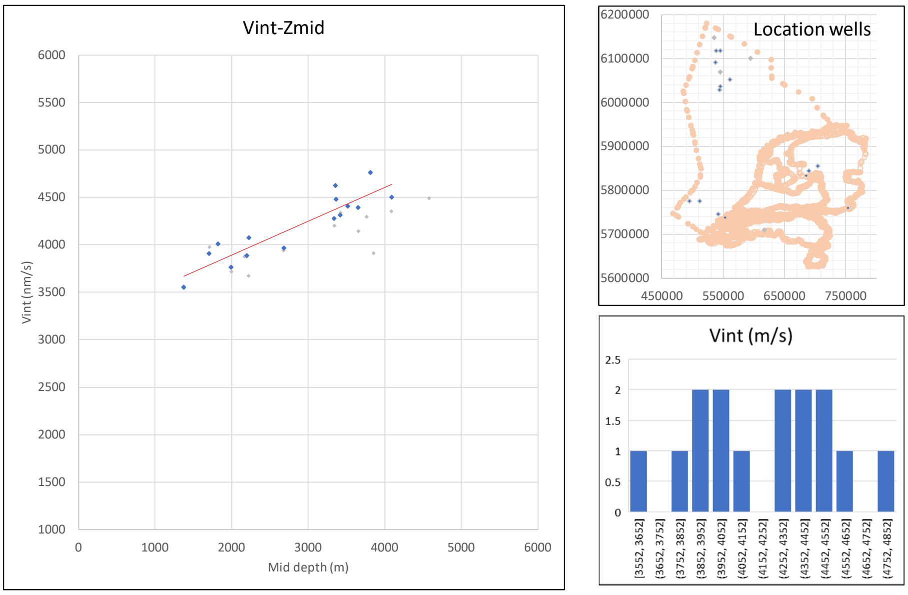

Figure 3.16 Interval velocity vs mid-depth (left; grey points are discarded from regression analysis), distribution (lower right) and location (upper right) of interval velocities of the Geul Subgroup (Namurian age).

3.4 Model parameterization of the Upper-Jurassic Supergroup

Specifically, for the Upper-Jurassic Supergroup a more detailed regression analysis was done, where we differentiated into different clusters of structural elements. This is shown in Figure 3.1, where we consider:

- S_all: well velocity data of all structural elements of the Upper-Jurassic Supergroup;
- S1: Lower Saxony Basin, Central Netherlands Basin, West Netherlands Basin and Broad Fourteens Basin;
- S2: Vlieland Basin, Terschelling Basin and Step Graben;
- S3: Dutch Central Graben.

Linear regression fits were made for the individual datasets of the three Upper Jurassic clusters, resulting in different k- and V_0 values per cluster. This differs from VELMOD3.1 where a manual fit with uniform k value (k=0.52) was made for all three Upper Jurassic clusters (see Pluymaekers et al. 2017). The equations of the different linear regression fits are shown where the slope and constant respectively represent the k and V_0-value, which are also listed in Table 3.1. This shows that the k- values for S1, S2 and S3 (respectively 0.52, 0.77 and 0.66) differ significantly from S_all (0.26). This may question the representativeness of using a uniform k-value for the entire Upper-Jurassic Supergroup when constructing a velocity model as we have done here. Region-specific k values should be considered on a regional scale, although care must be taken, because the data size for S2 and S3 is rather limited compared to S1. This makes the regression analysis for these two clusters less robust and increases its uncertainty. Based on statistical analysis from Pluymaekers et al. (2017) there appeared limited statistical significance to treat the three Upper Jurassic clusters separately. Therefore, for the generation of V_{int} and V_0 maps and grids we treated the Upper-Jurassic Supergroup as a uniform entity, like Pluymaekers et al. (2013).

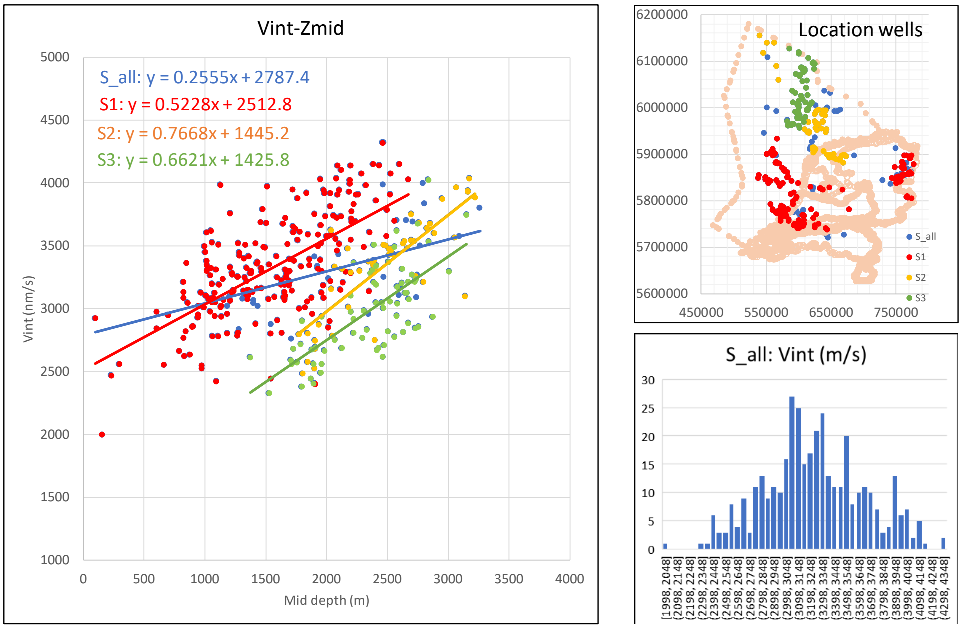

Figure 3.1 More detailed regression analysis for the Upper-Jurassic Supergroup, with differentiation into different structural element clusters. S_all: all well data of Upper-Jurassic Supergroup, S1: Lower Saxony Basin, Central Netherlands Basin, West Netherlands Basin and Broad Fourteens Basin; S2: Vlieland Basin, Terschelling Basin and Step Graben; S3: Dutch Central Graben. The equations of the different regression fits are shown where the slope and constant respectively represent the k and V_0-value, which are also listed in Table 3.1. The location of used well data for the different structural element clusters is shown in the upper right figure. The distribution of interval velocities for all datapoints of the Upper-Jurassic Supergroup in the lower right figure.

3.5 Model parameterization of Zechstein and other Paleozoic groups

The lithology of the Zechstein Group in general consists of anhydrite, halite, and/or carbonate. The lithological composition of the interval is the most dominant factor for the interval velocity. The influence of compaction on the interval velocity is considered very minor. The Zechstein interval velocity is modelled based on velocity – one-way-time (ΔT) relation from wells (**Fout! Verwijzingsbron niet gevonden.**). In general, layers with limited thickness show the relative high abundance of high velocity carbonate layers (Kombrink et al, 2012). The trend line in **Fout! Verwijzingsbron niet gevonden.** is described by:

$$V_{int\ prov} = 4500\ m/s \qquad if\ \Delta t_{ZE} \geq 170\ ms$$
$$V_{int\ prov} = 4950 - 450.\cos(\Delta t_{ZE} + 10) \qquad if\ \Delta t_{ZE} < 170\ ms$$

The final V_{int}-grid was obtained by kriging the difference (V_{int} prov – V_{int} borehole) at borehole locations, and by subtracting the kriged differences from the V_{int}prov-grid. In this step the minimum V_{int}-value in the final velocity grid was constrained to 4400 m/s.

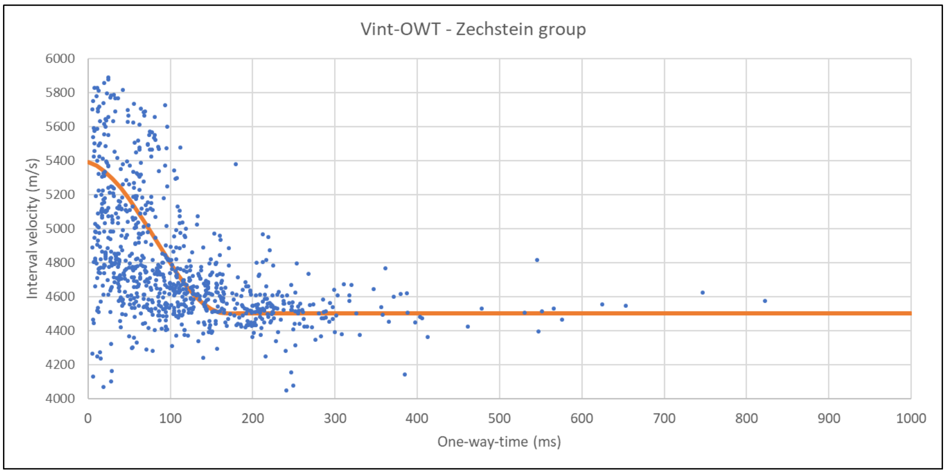

Figure 3.2 Interval velocity Vint in relation to thickness (ΔT-ZE in ms OWT=One-Way-Time) for Zechstein Group.

Interval velocities of other Paleozoic lithostratigraphic groups were processed. Because of the limited amount of data, no velocity depth trend was derived for these intervals. For completeness the data points are shown in Figure 3.3 to Figure 3.6 and a data overview is given in Table 3.1.

Table 3.1 Overview of data availability of in general non-compacting lithostratigraphic group (Zechstein) and groups with a very limited dataset.

Strat	Area	# Boreholes
ZE	Dutch territory	854
RV	Dutch territory	9
CL	Dutch territory	7
CF	Dutch territory	2

ZE

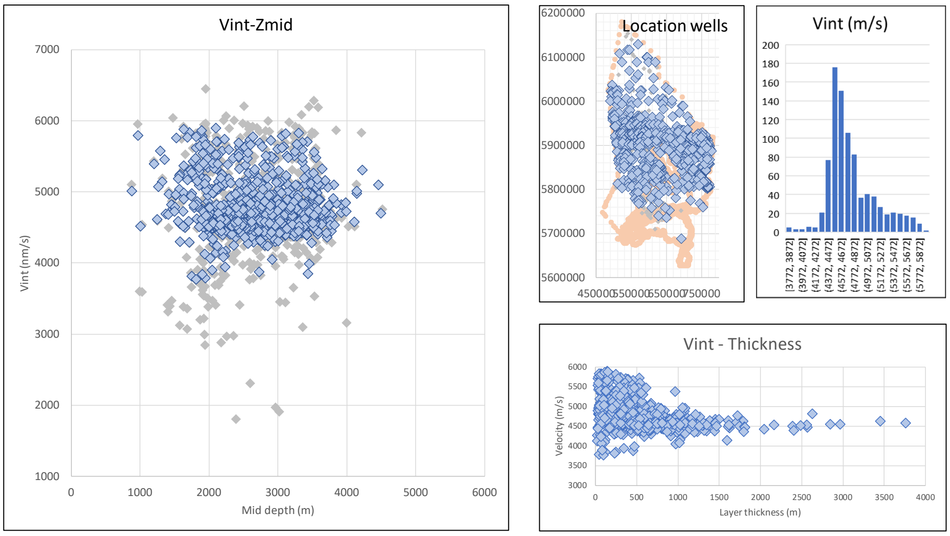

Figure 3.3 Interval velocity vs mid-depth (left), location of wells (upper centre right), distribution & location (upper right) of interval velocities and interval velocity vs thickness (lower right) of the Zechstein Group. Note that the grey points were discarded during data selection and not used for further analysis.

RV

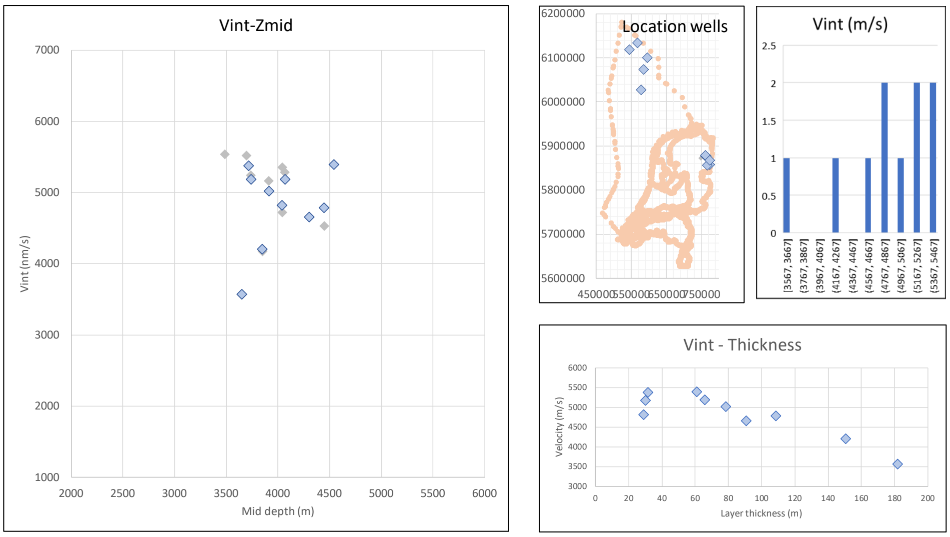

Figure 3.4 Interval velocity vs mid-depth (left), location of wells (upper centre right), distribution & location (upper right) of interval velocities and interval velocity vs thickness (lower right) of the Lower Rotliegend Group. Note that the grey points were discarded during data selection and not used for further analysis.

CL

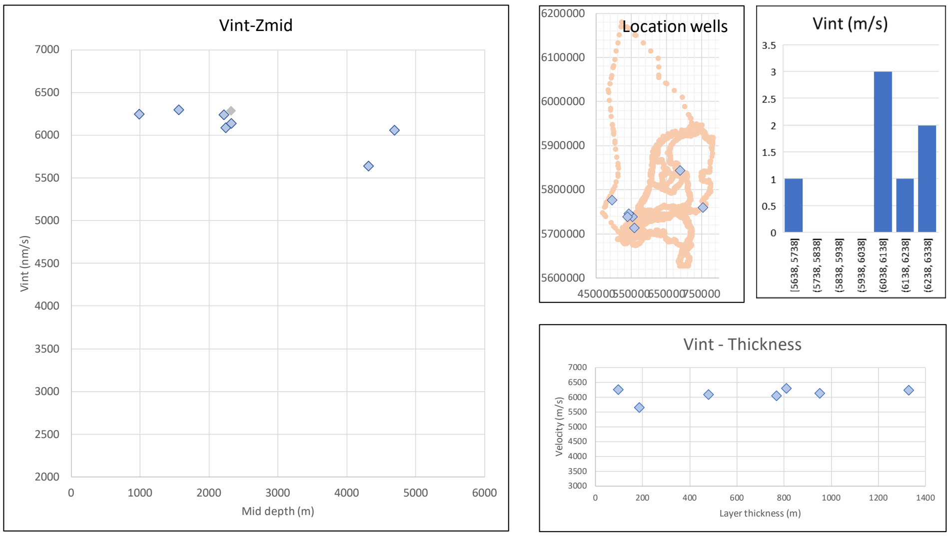

Figure 3.5 Interval velocity vs mid-depth (left), location of wells (upper centre right), distribution & location (upper right) of interval velocities and interval velocity vs thickness (lower right) of the Carboniferous Limestone Group (Dinantian age). Note that the grey points were discarded during data selection and not used for further analysis.

CF

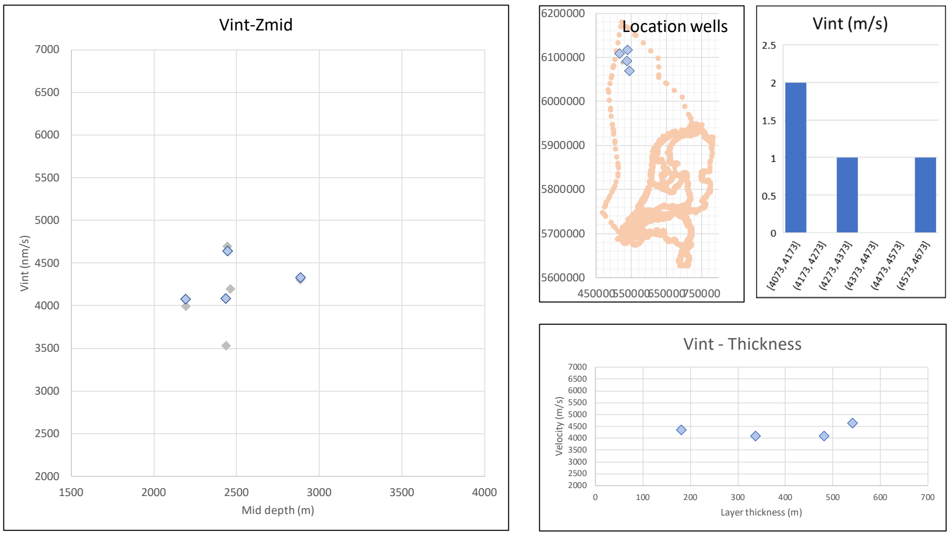

Figure 3.6 Interval velocity vs mid-depth (left), location of wells (upper centre right), distribution & location (upper right) of interval velocities and interval velocity vs thickness (lower right) of the Farne Group (Dinantian age, clastic sediments). Note that the grey points were discarded during data selection and not used for further analysis.

4 Results

4.1 Spatial data analysis

Similarly to VELMOD-3.1, regional V_0 distribution maps were constructed based on parameterization of V_0 and k using the local basefit calibration method of Japsen (1993). Here the total vertical travel time ΔT of the sonic data from top to base of a layer (z_t and z_b) is used:

$$V_0 = \frac{k\,(Z_b - Z_t\, e^{k\Delta T})}{e^{k\Delta T} - 1} \qquad \text{(eq. 2)}$$

Gridding of the V_{int} and V_0 data points was conducted with Petrel modelling software. The grid cell size is 1000m x 1000m and standard kriging was applied. A spherical variogram model was used with a relative nugget of 10% of the total variance. Variogram ranges were adopted from the findings of VELMOD-3.1, which was obtained through exploratory data analysis (Isatis statistic software). Used variogram ranges are listed in Table 4.1.

Table 4.1. Derived variogram ranges.

Strat interval	range V_{int} [km]		range V_0 [km]
N	60		25
NU	40		25
NM+NL	100		35
CK	75		45
KN	60		60
KNGL	77		32
KNN	50		50
S	45		54
AT	55		50
RN+RB	50		55
RN	50		45
RB	50		60
RO	55		60
DC	50		20

4.2 Regional V_{int} distribution maps

Resulting V_{int} distribution grids are depicted in Figure 4.1 to Figure 4.15, which show the gridded interval velocity of a stratigraphic group at its mid-depth. The related kriging standard deviation maps are shown in appendix B.
In general interval velocities increase with depth due to compaction of the rocks.

Furthermore, time-depth pairs were generated from the processed velocity files for the base of every stratigraphic interval, which are given in Appendix C.

Note that specifically for the Zechstein - and the Upper Rotliegend Groups the interval velocity (Figure 4.13 and Figure 4.14) is harder to map and less reliable at areas where the Zechstein Group becomes very thin (<20 m), such as the southern part of the Netherlands and along the boundary of the Elbow Spit High (also see ten Veen et al., 2012).

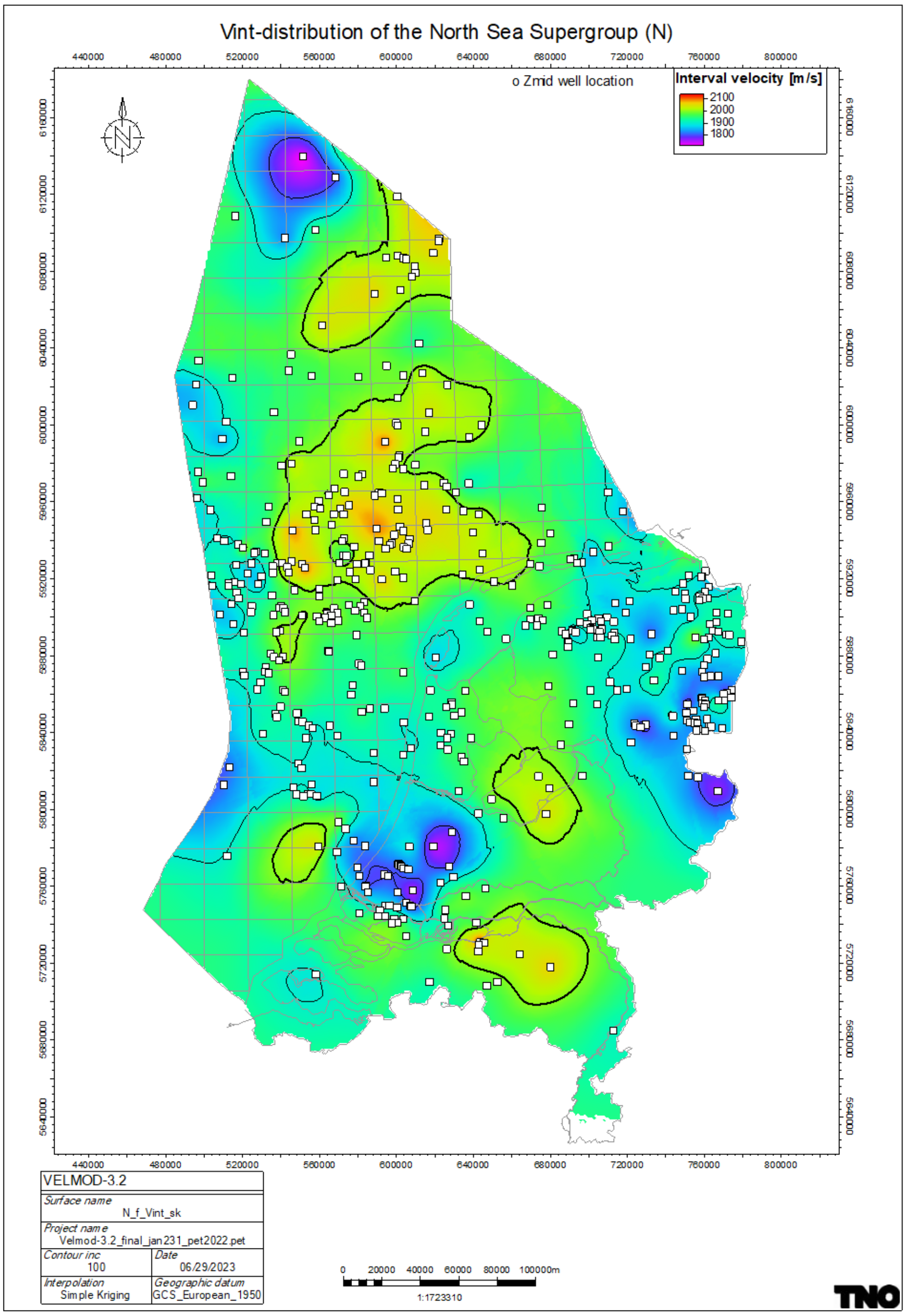

Figure 4.1 V_{int} distribution of the North Sea Supergroup.

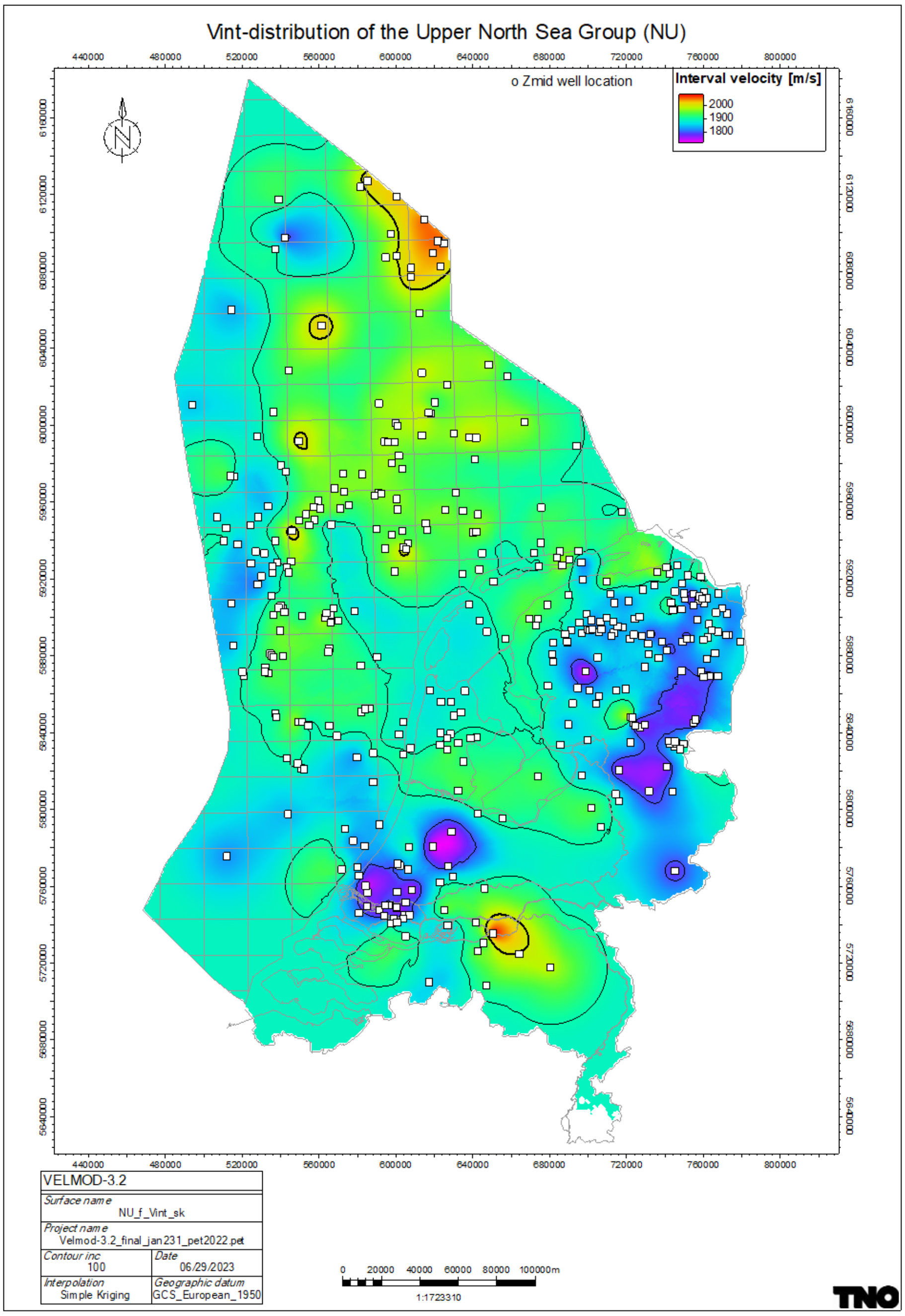

Figure 4.2 V_{int} distribution of the Upper North Sea Group.

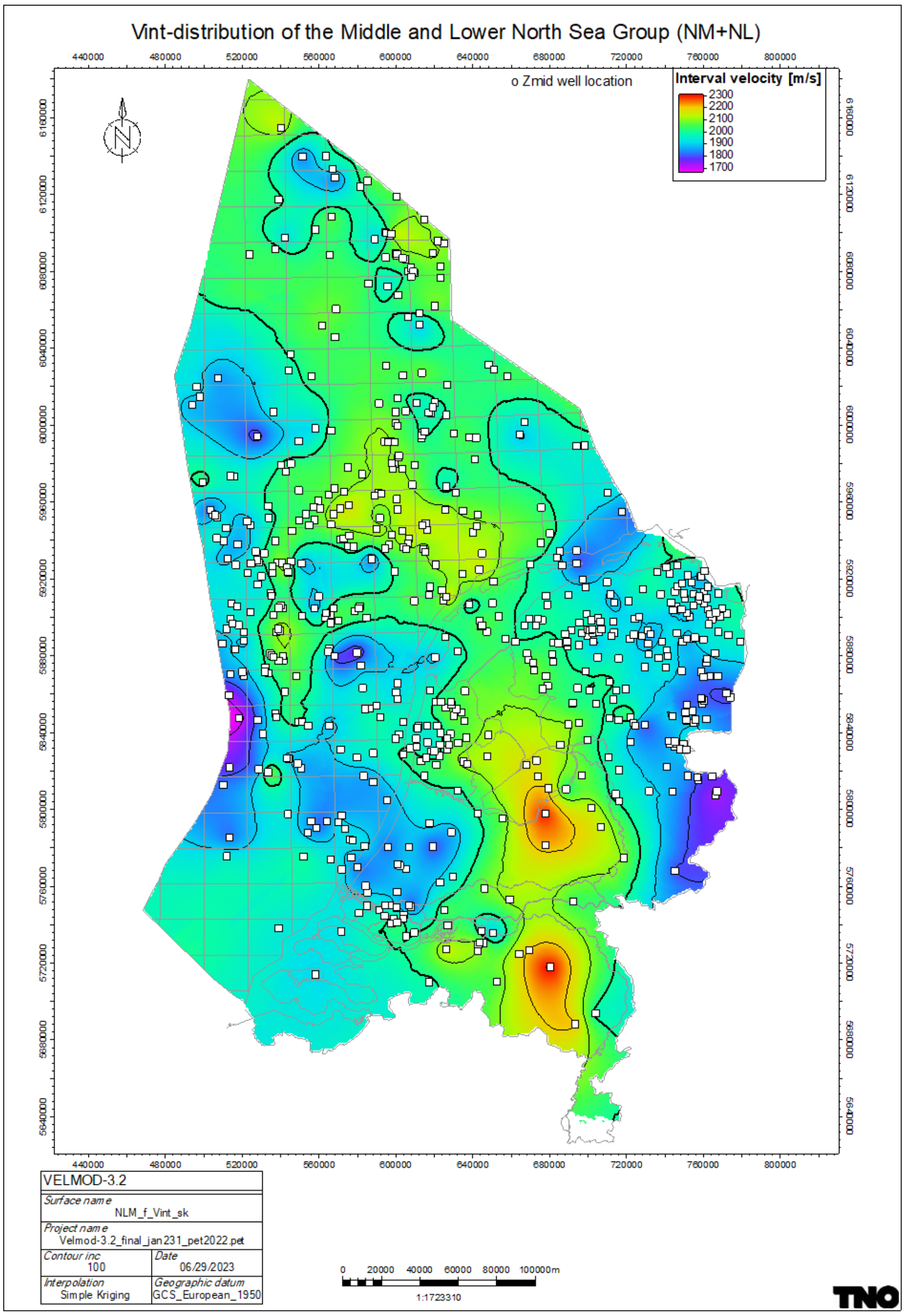

Figure 4.3 V_{int} distribution of the Middle- and Lower North Sea groups.

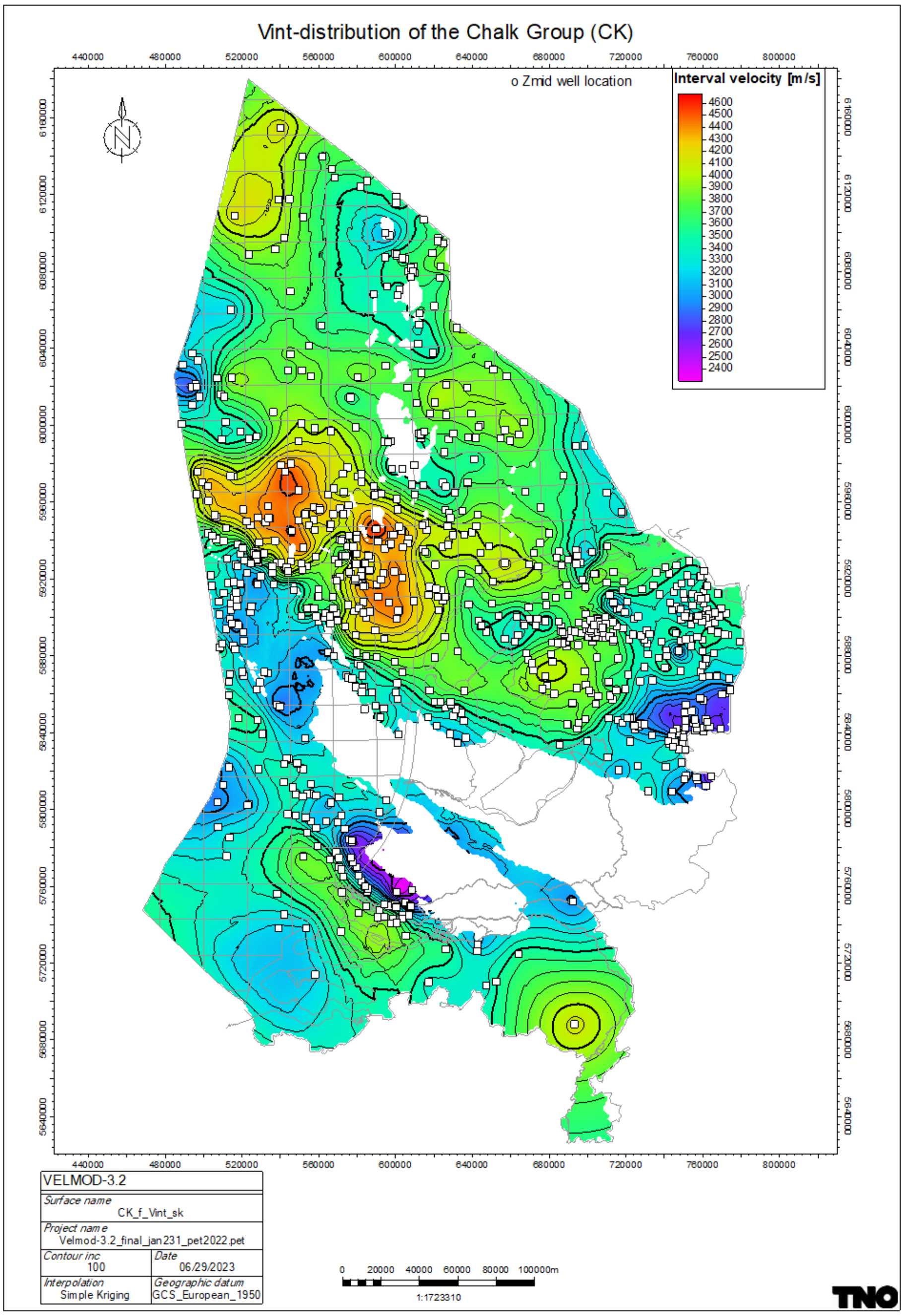

Figure 4.4 V_{int} distribution of the Chalk Group.

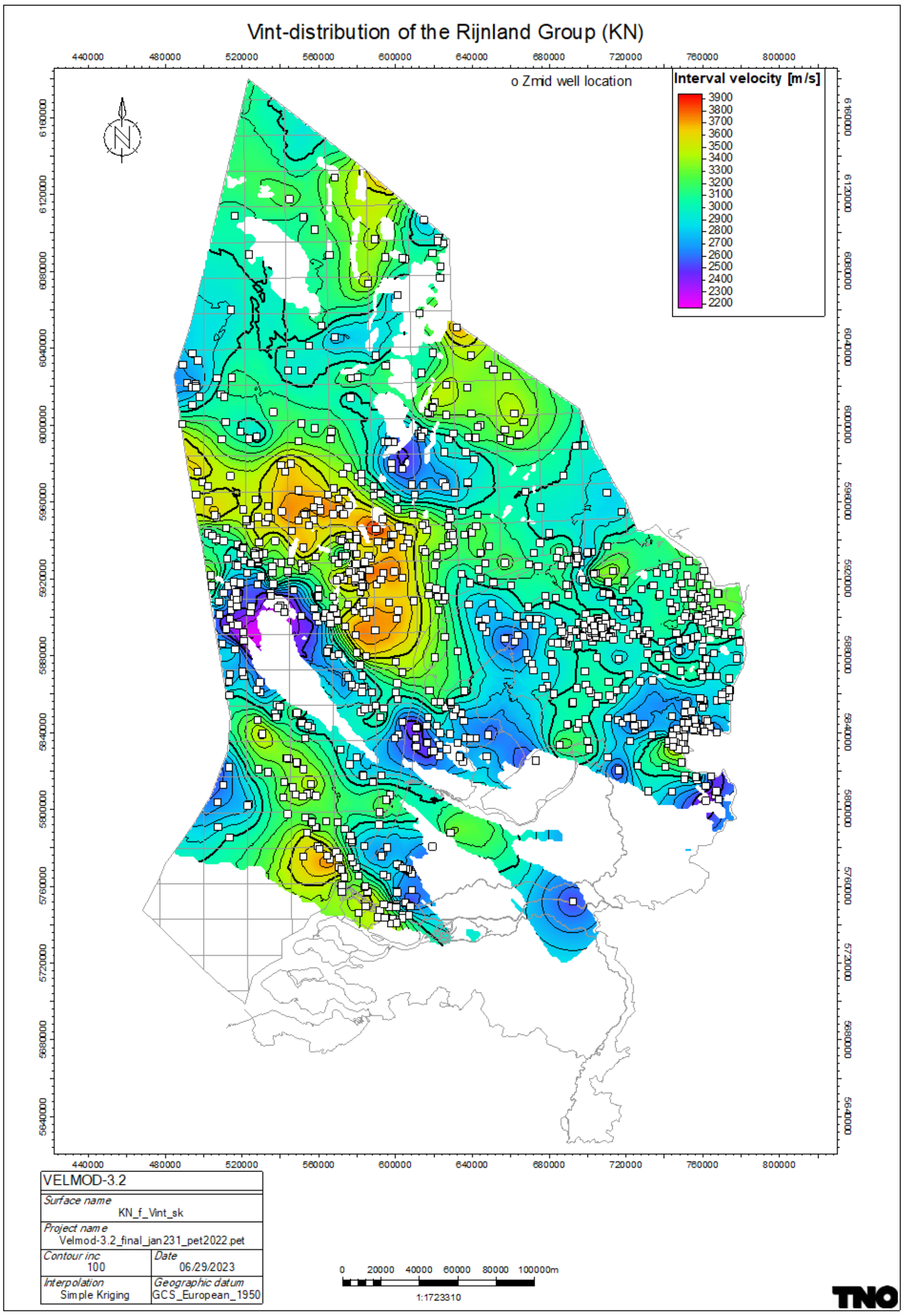

Figure 4.5 V_{int} distribution of the Rijnland Group.

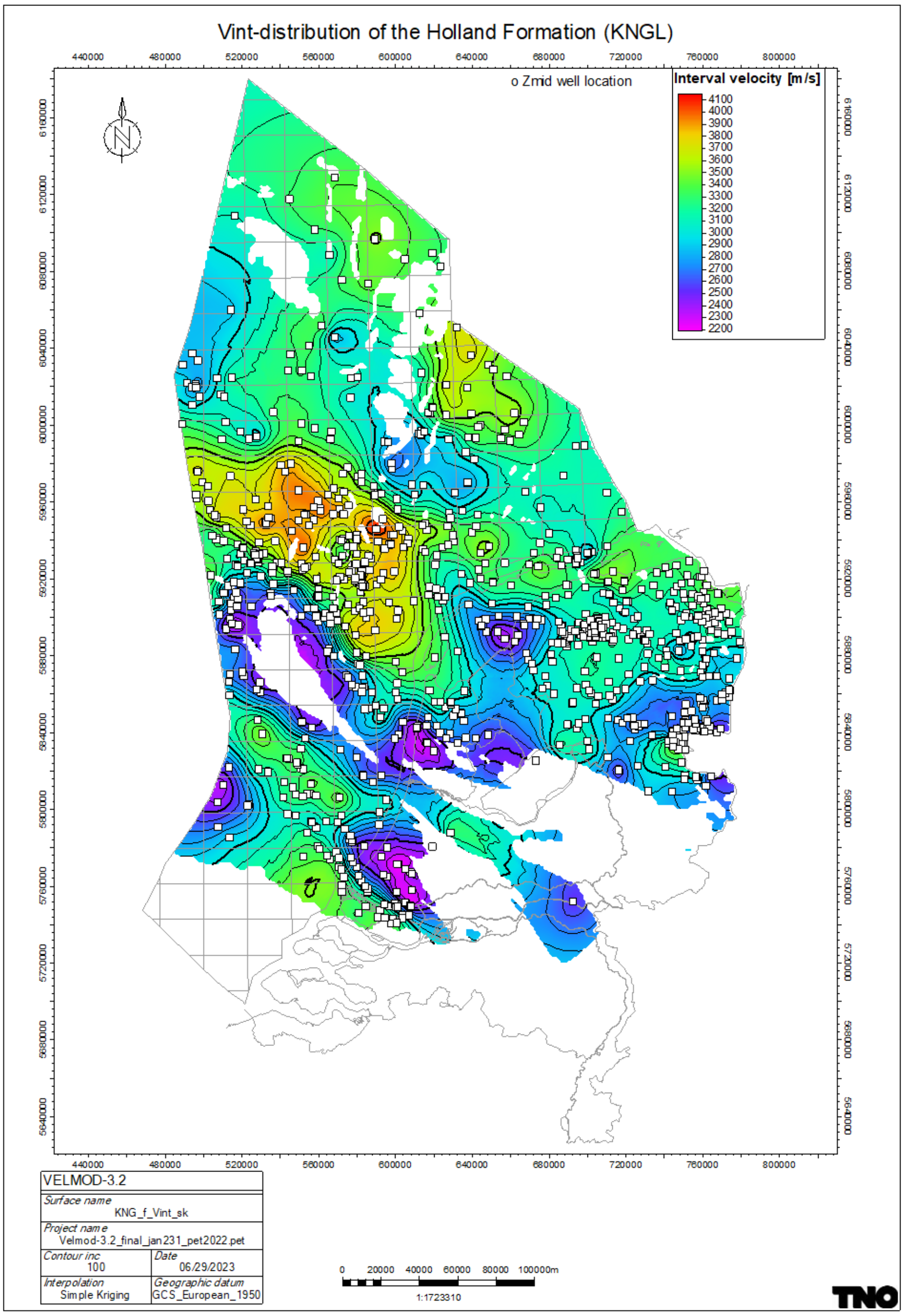

Figure 4.6 V_{int} distribution of the Holland Formation.

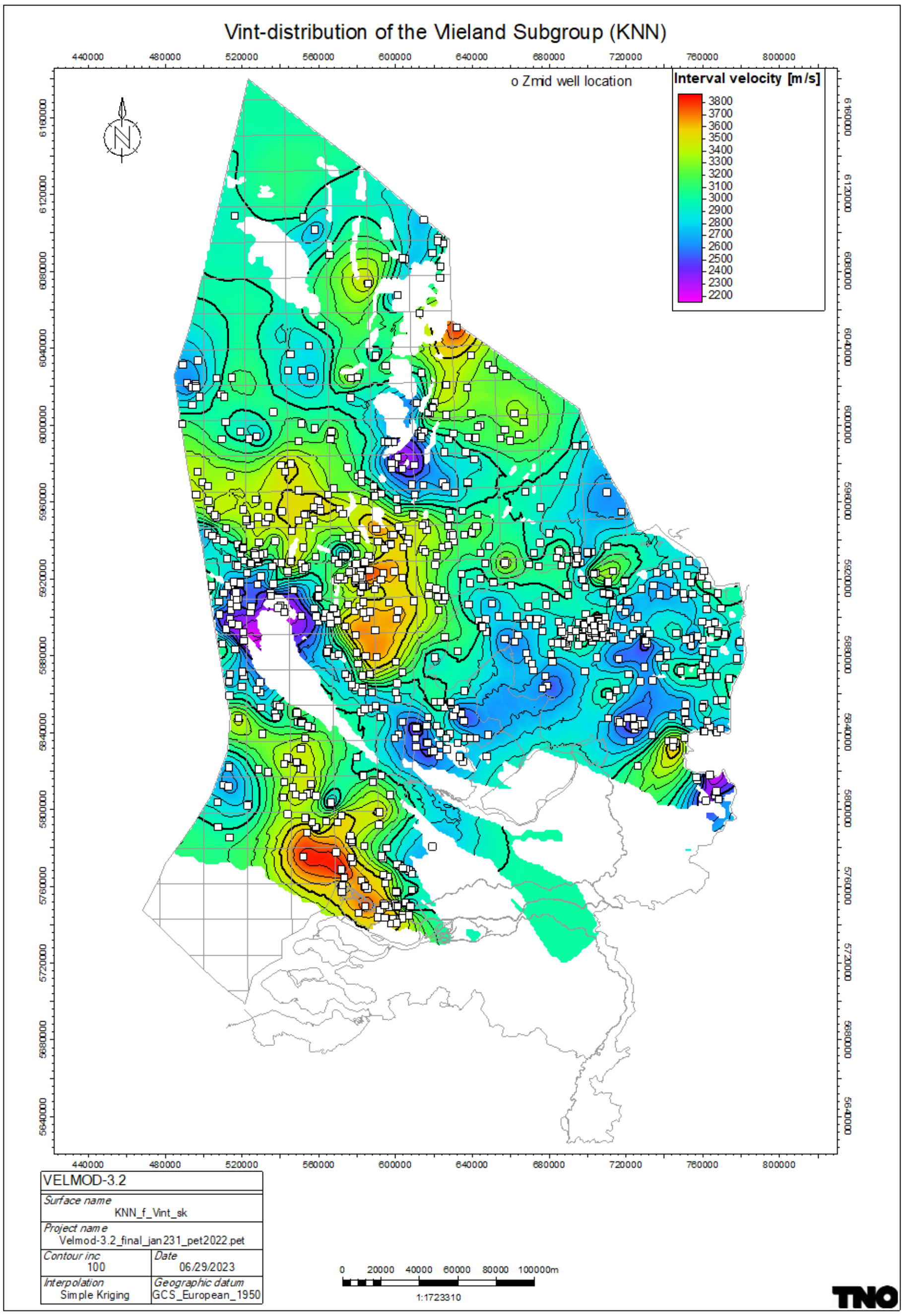

Figure 4.7 V_{int} distribution of the Vlieland Subgroup.

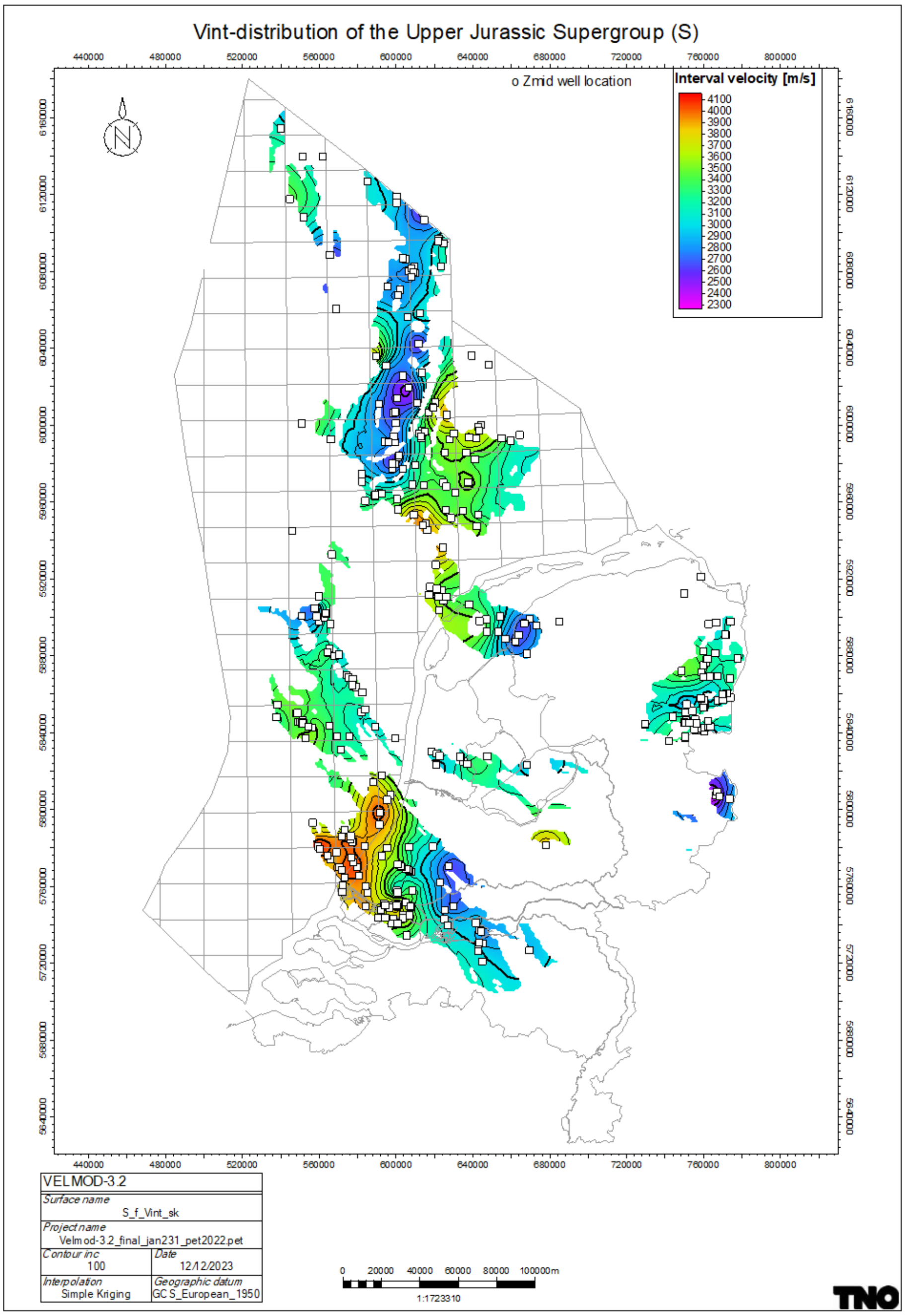

Figure 4.8 V_{int} distribution of the Upper-Jurassic Supergroup.

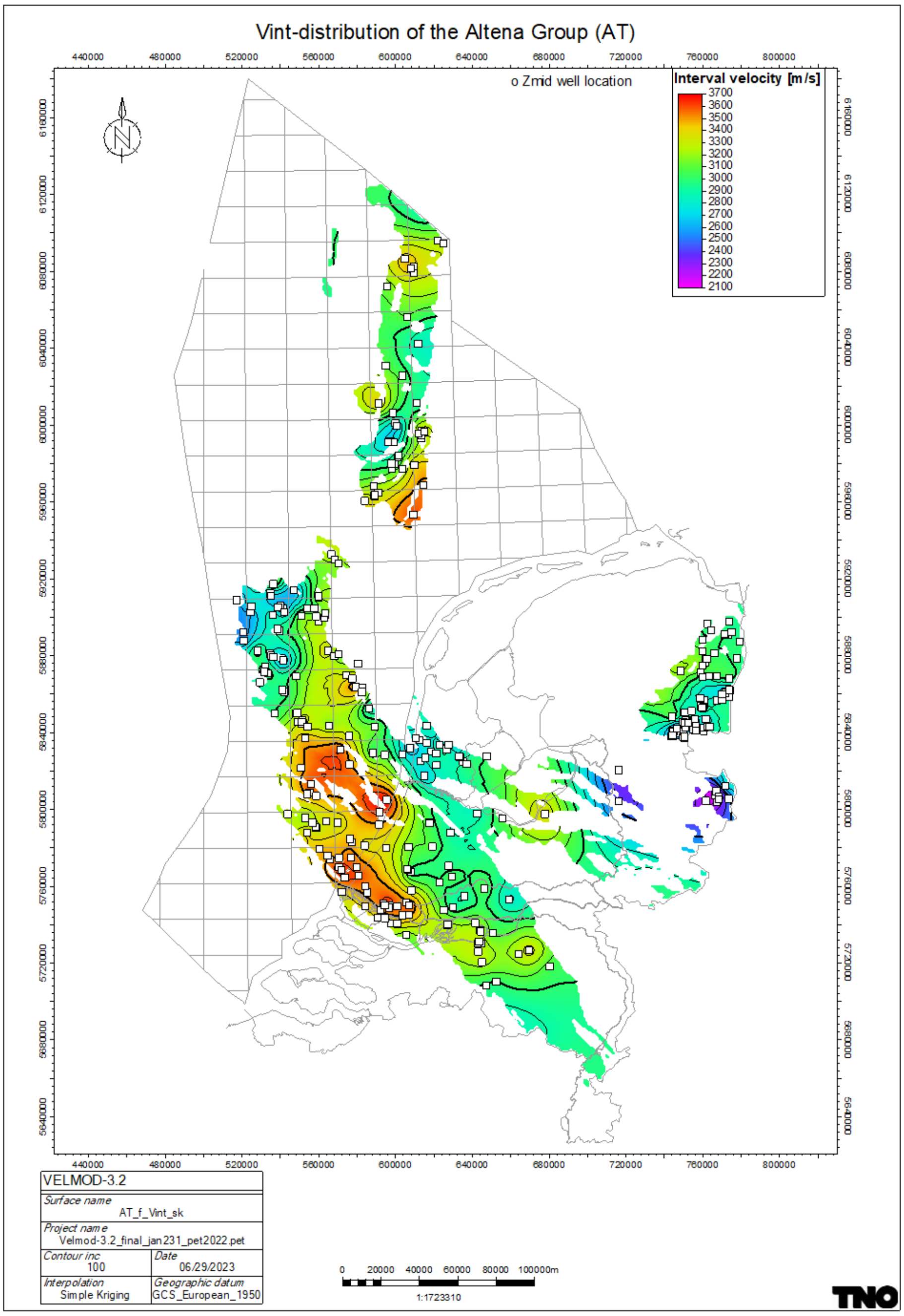

Figure 4.9 V_{int} distribution of the Altena Group.

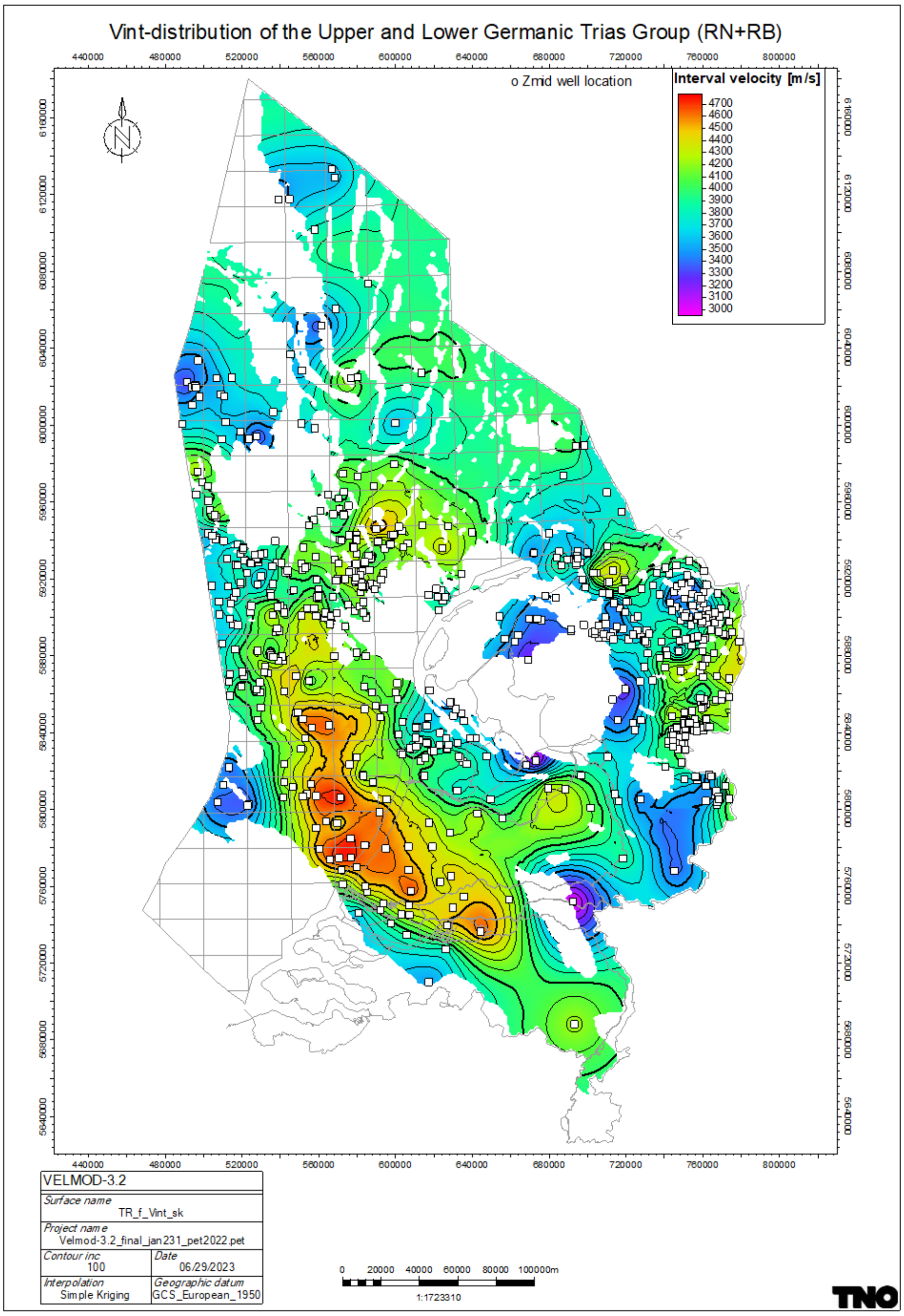

Figure 4.10 V_{int} distribution of the Upper and Lower Germanic Trias groups.

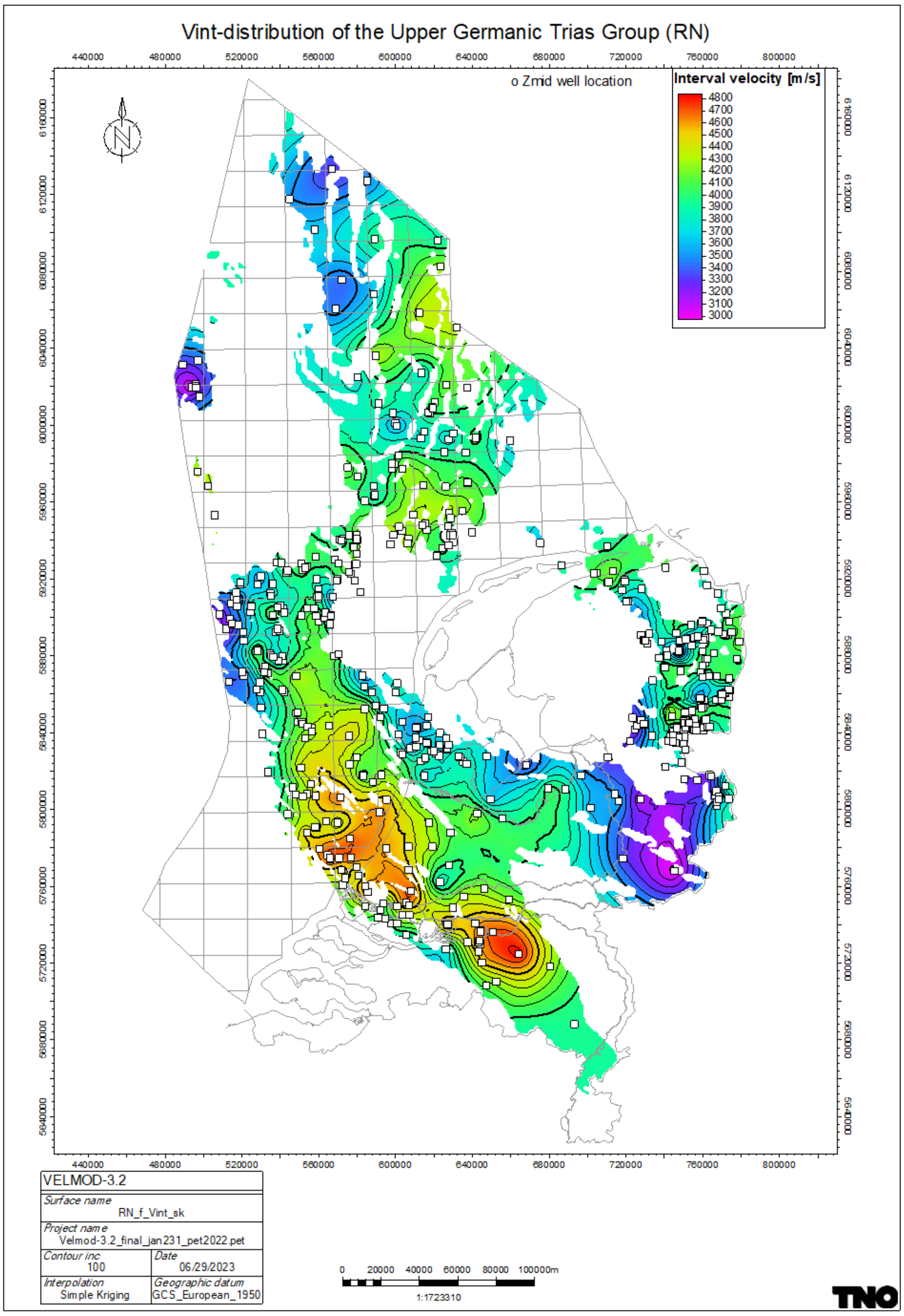

Figure 4.11 V_{int} distribution of the Upper Germanic Trias Group.

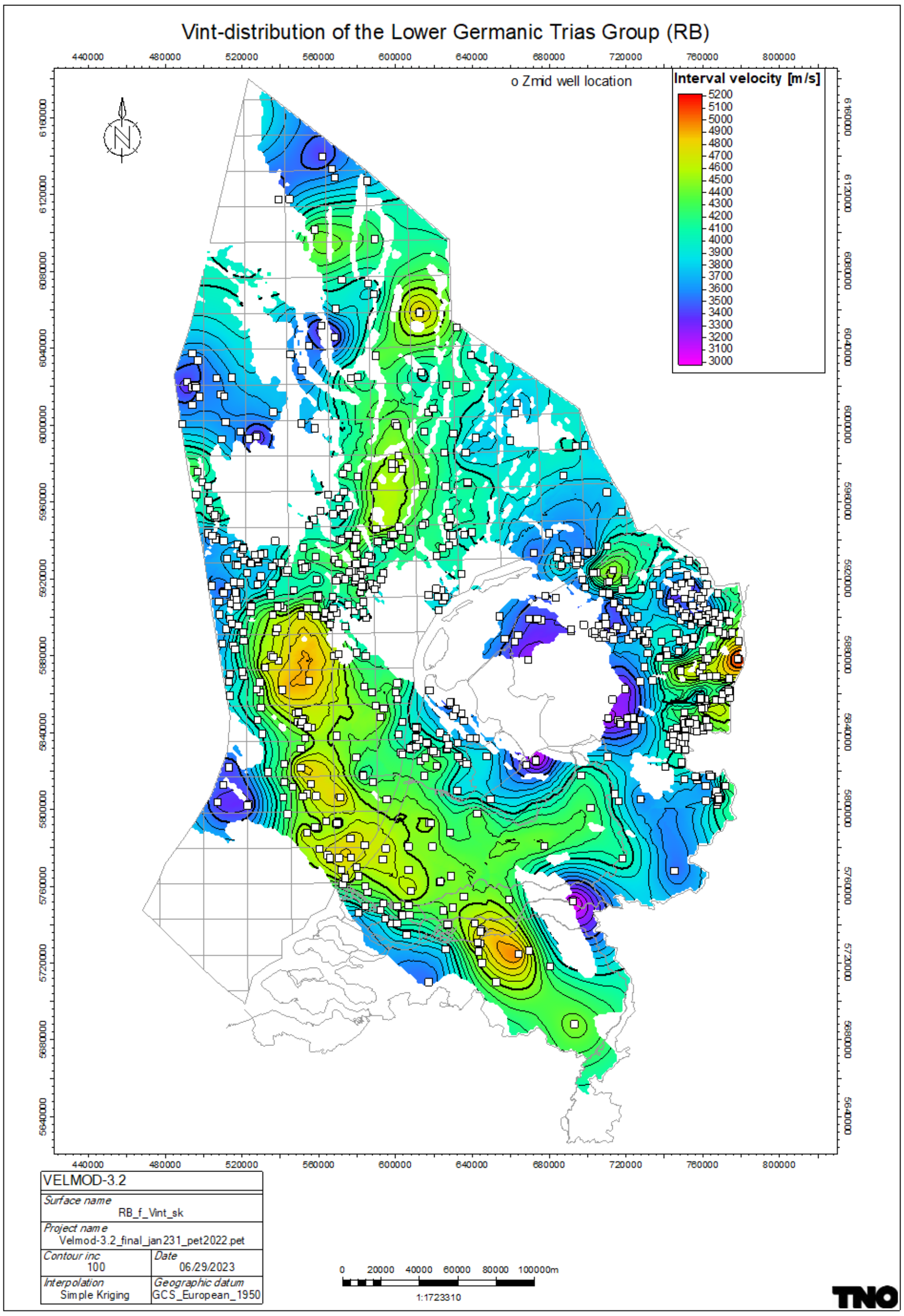

Figure 4.12 V_{int} distribution of the Lower Germanic Trias Group.

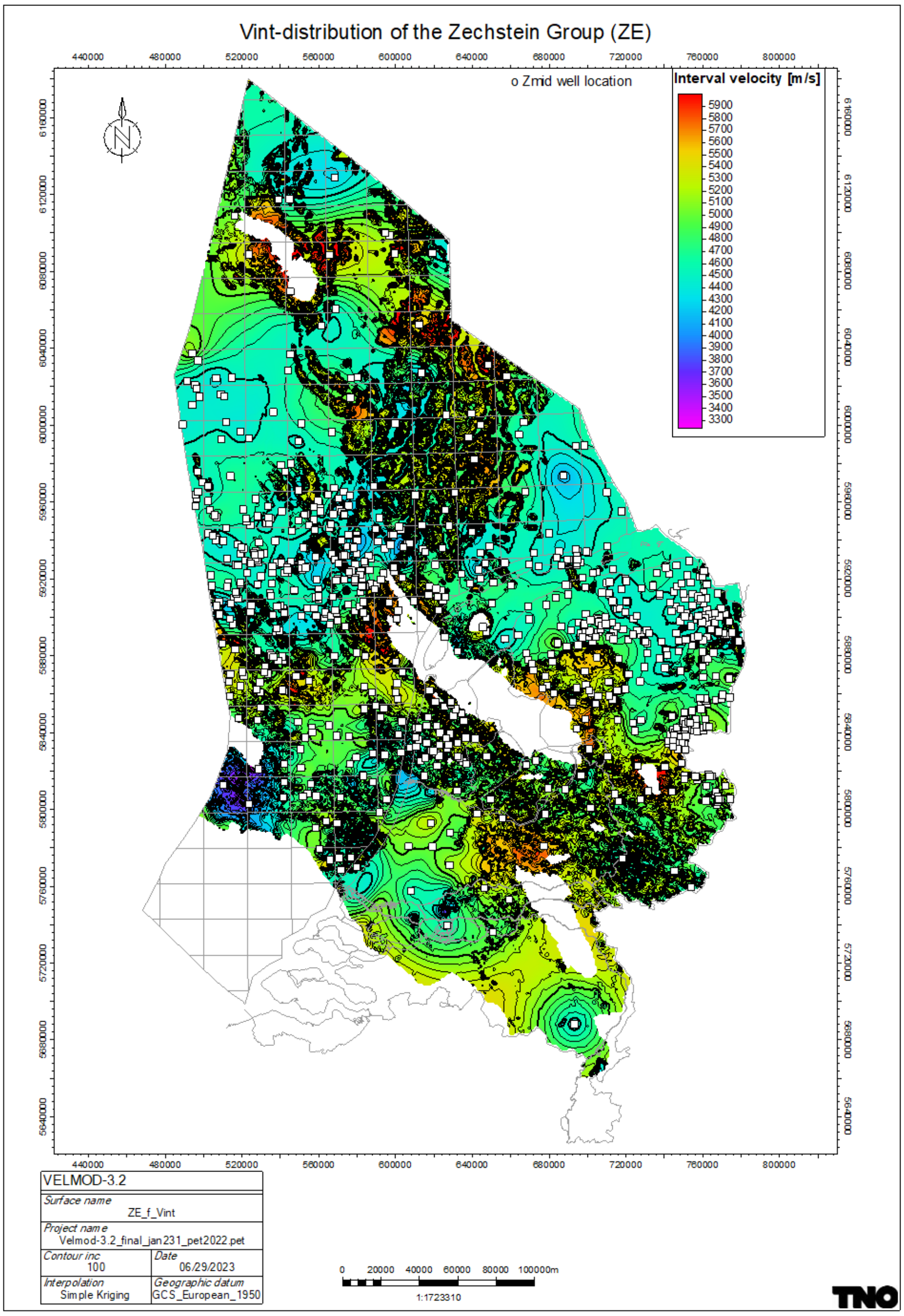

Figure 4.13 V_{int} distribution of the Zechstein Group.

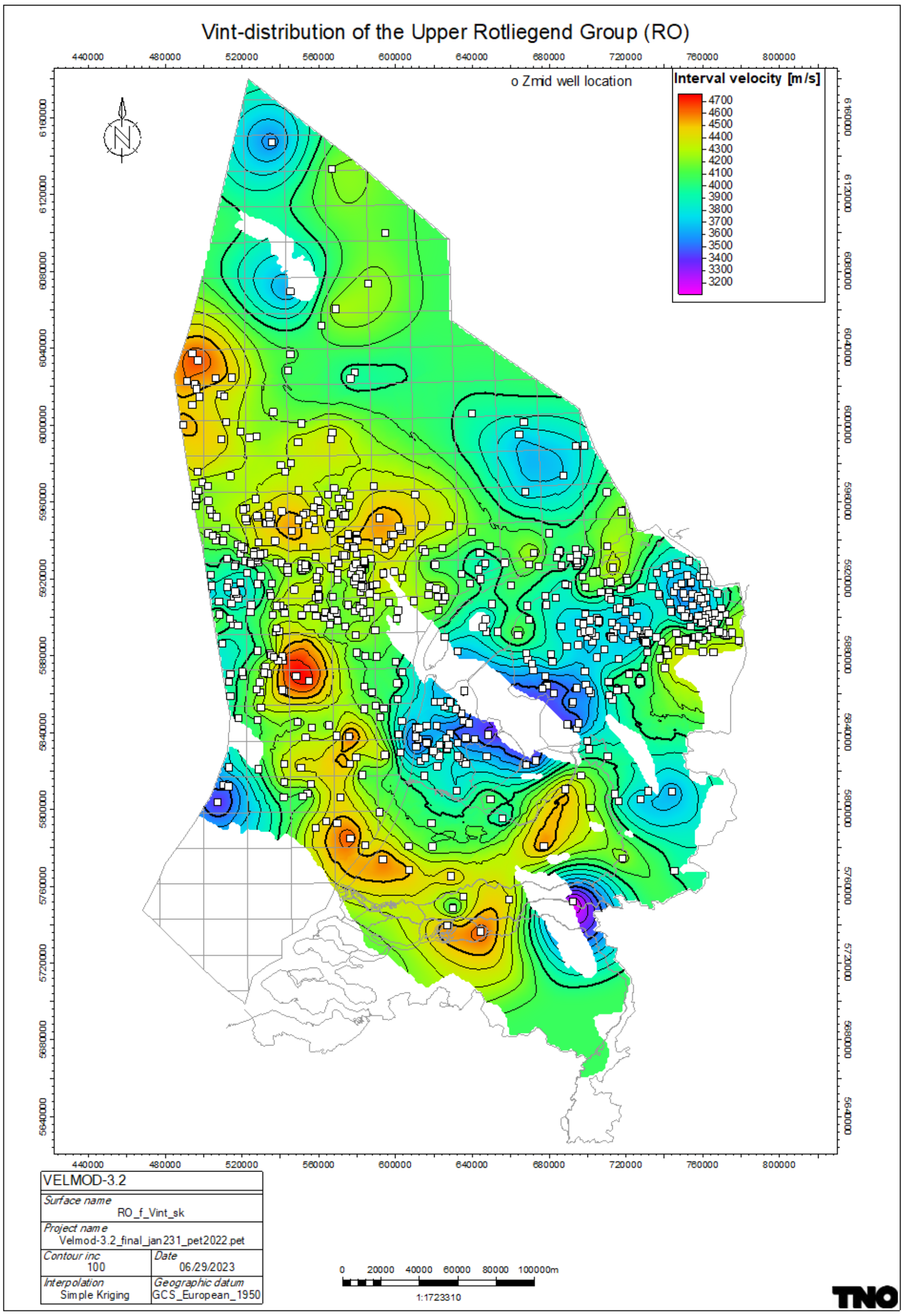

Figure 4.14 V_{int} distribution of the Upper Rotliegend Group.

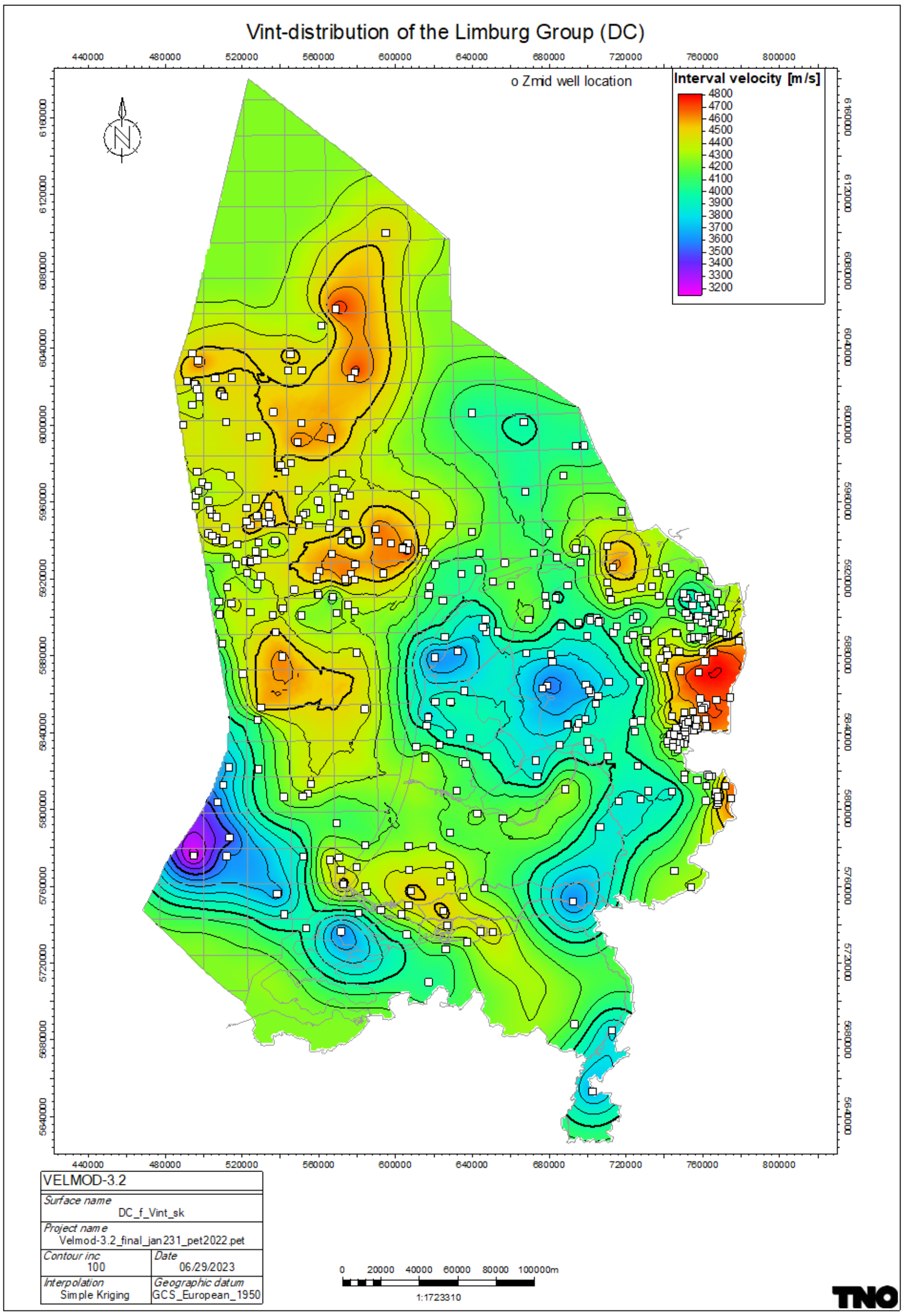

Figure 4.15 V_{int} distribution of the Limburg Group.

4.3 Regional V_0 distribution maps

Resulting V_0 distribution grids are shown in Figure 4.1 to Figure 4.14. The related kriging standard deviation maps are shown in appendix B.

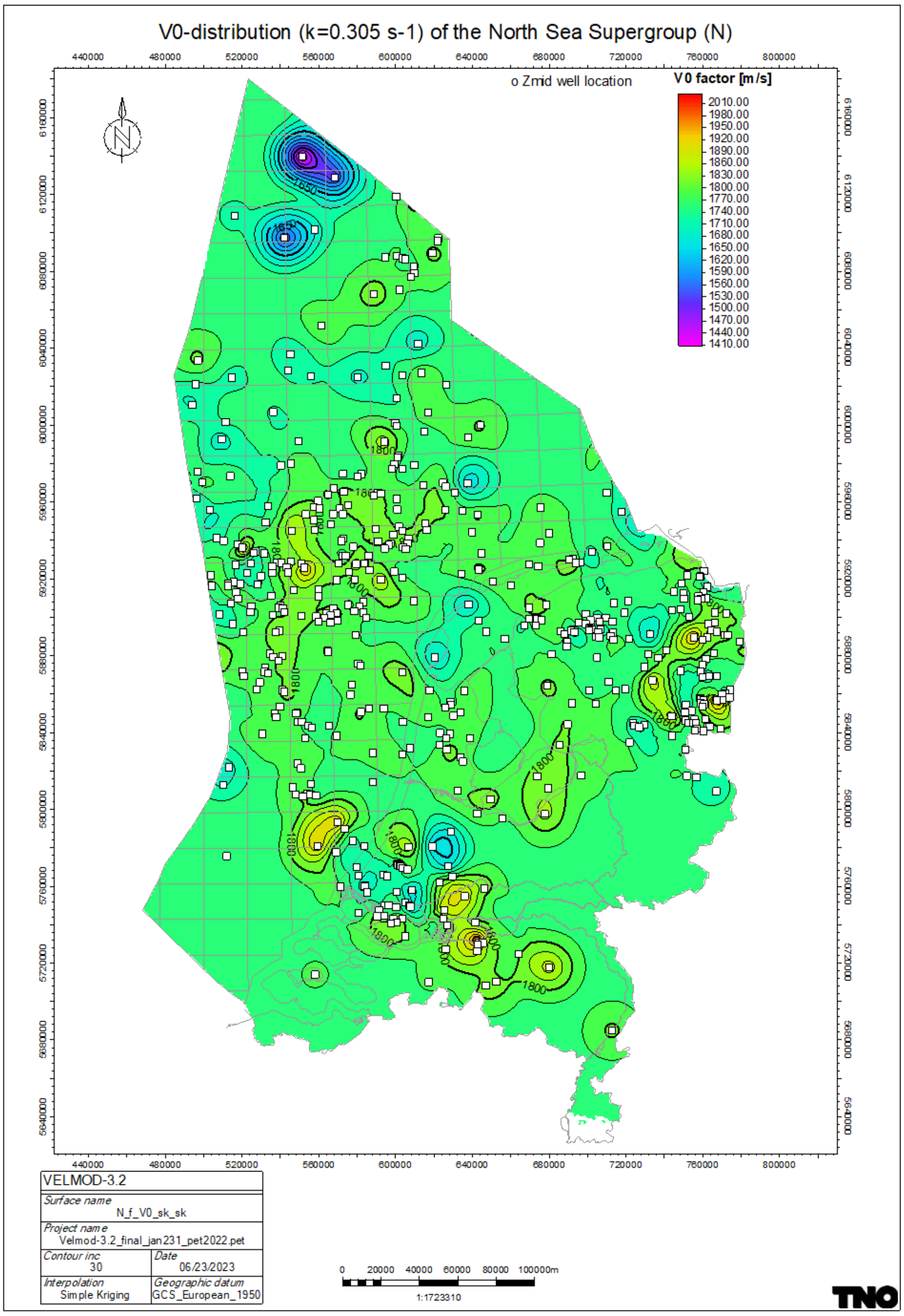

Figure 4.1 V_0 distribution of the North Sea Supergroup.

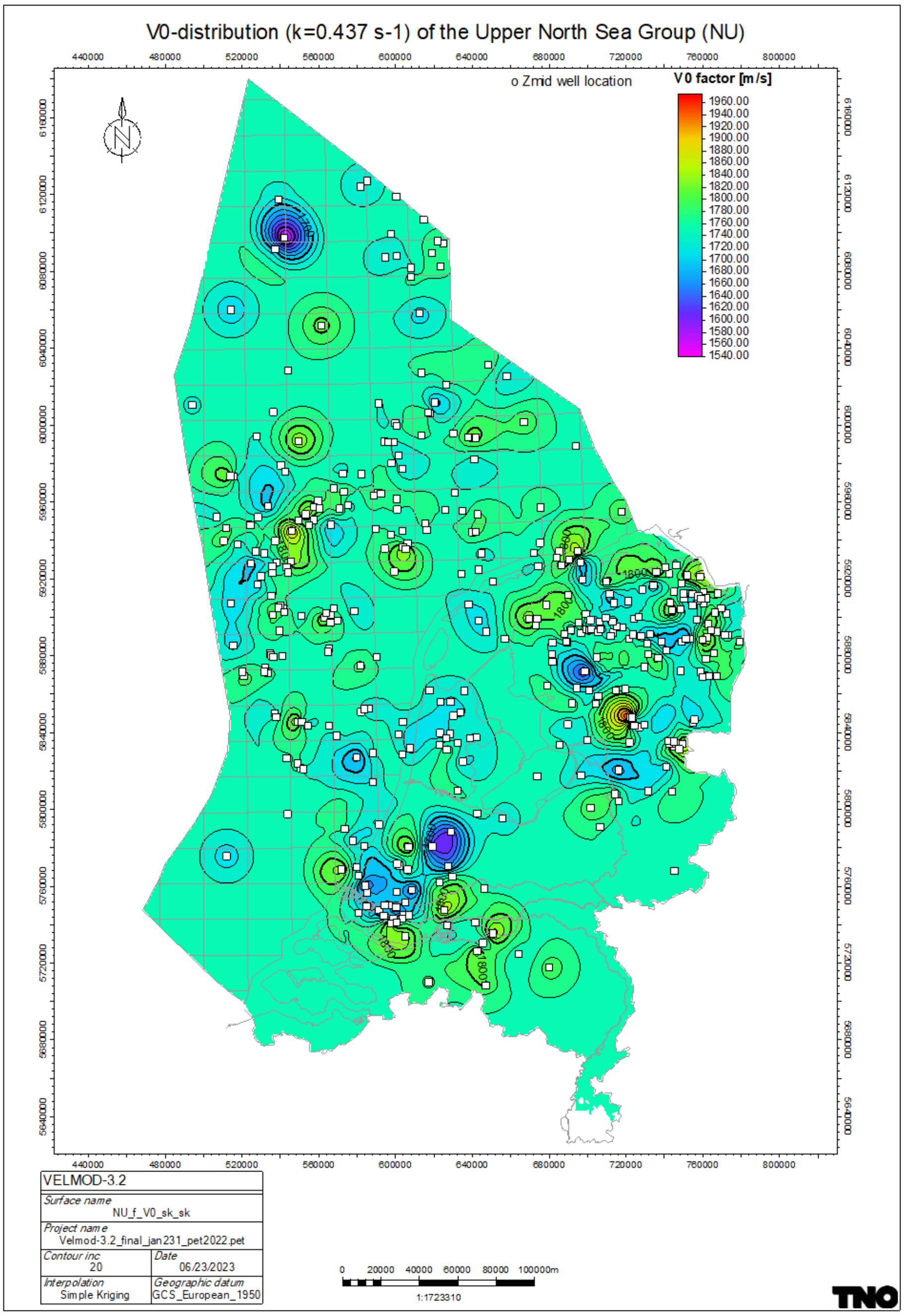

Figure 4.2 V_0 distribution of the Upper North Sea Group.

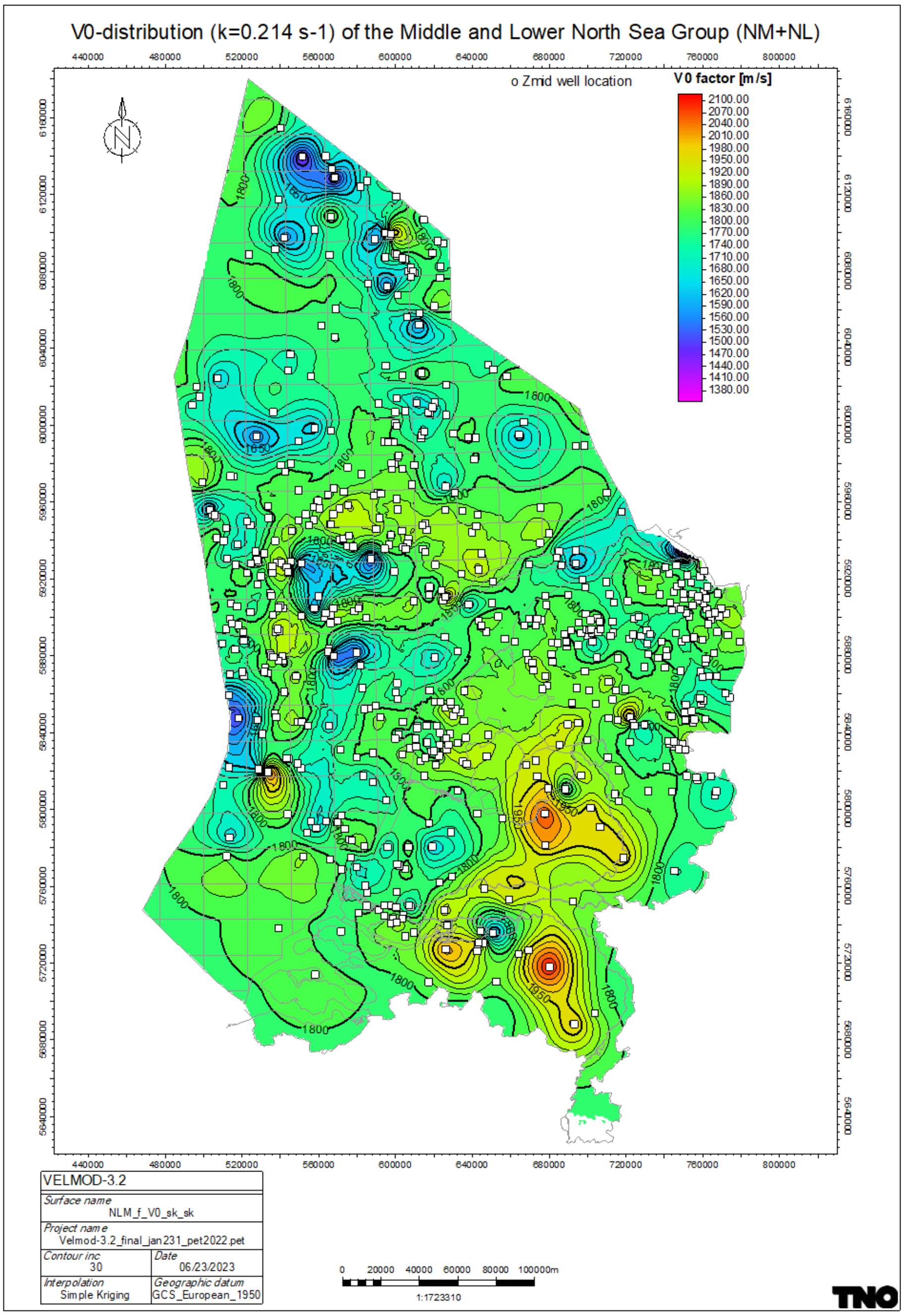

Figure 4.3 V_0 distribution of the Lower and Middle North Sea groups.

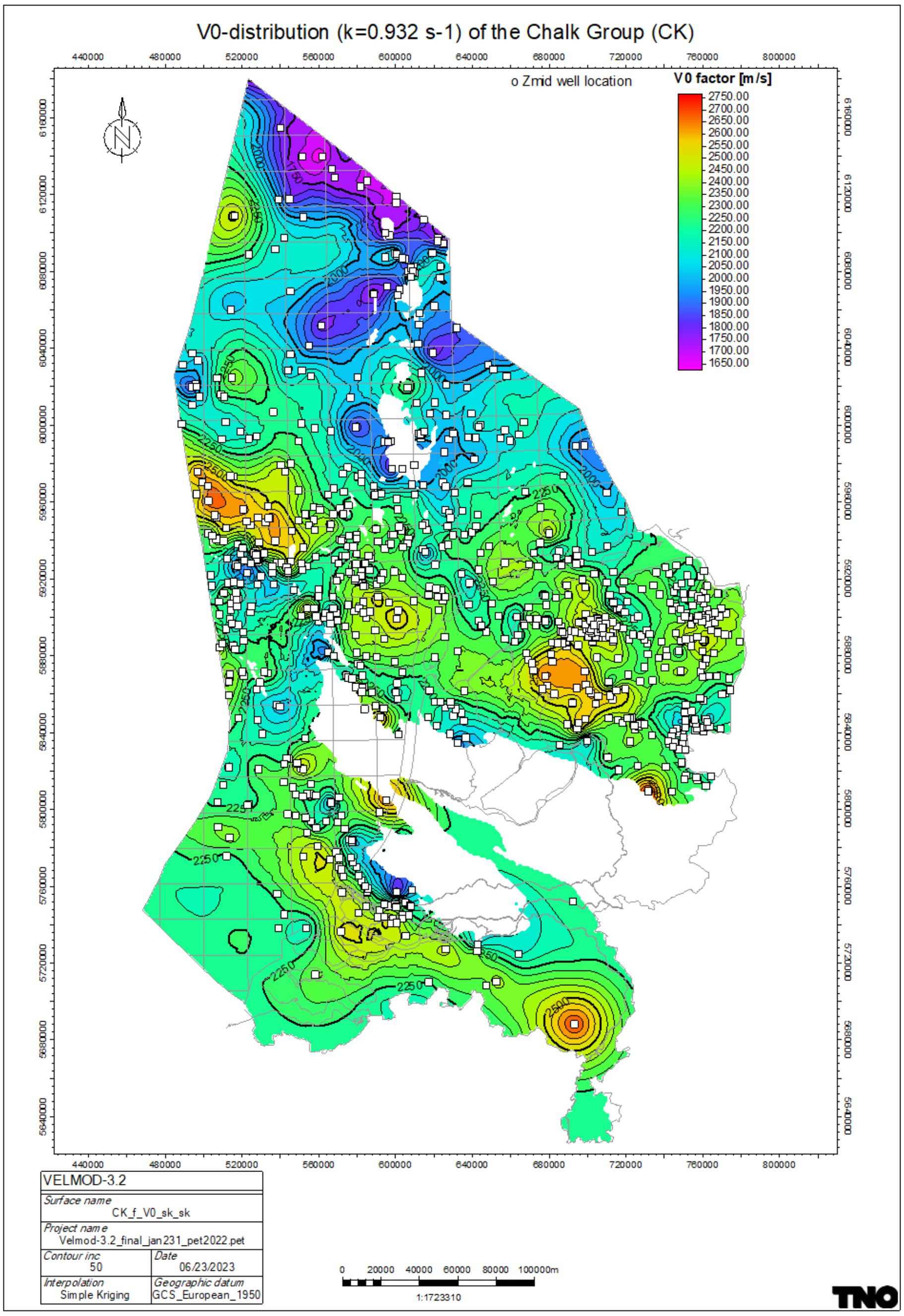

Figure 4.4 V_0 distribution of the Chalk Group.

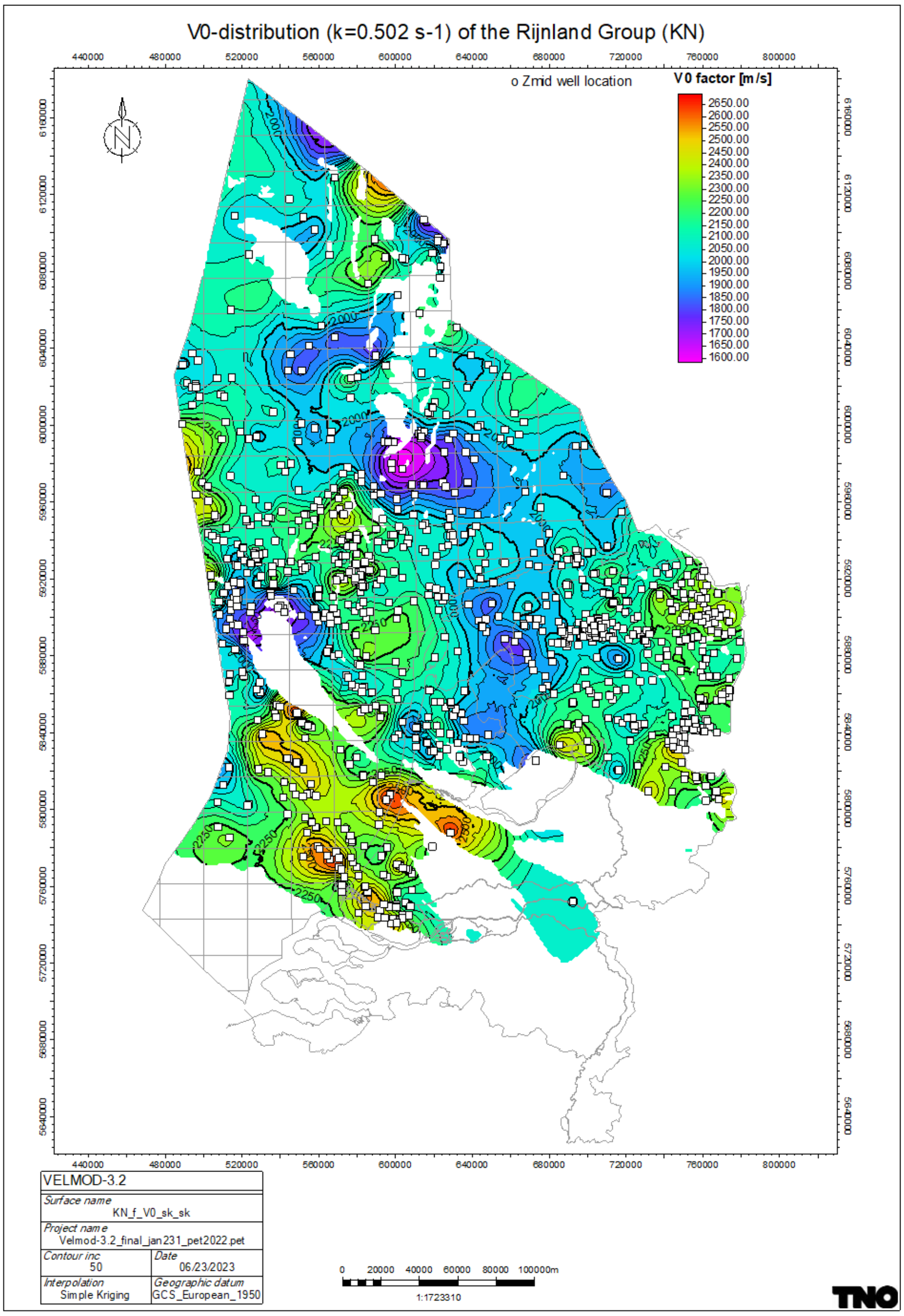

Figure 4.5 V_0 distribution of the Rijnland Group.

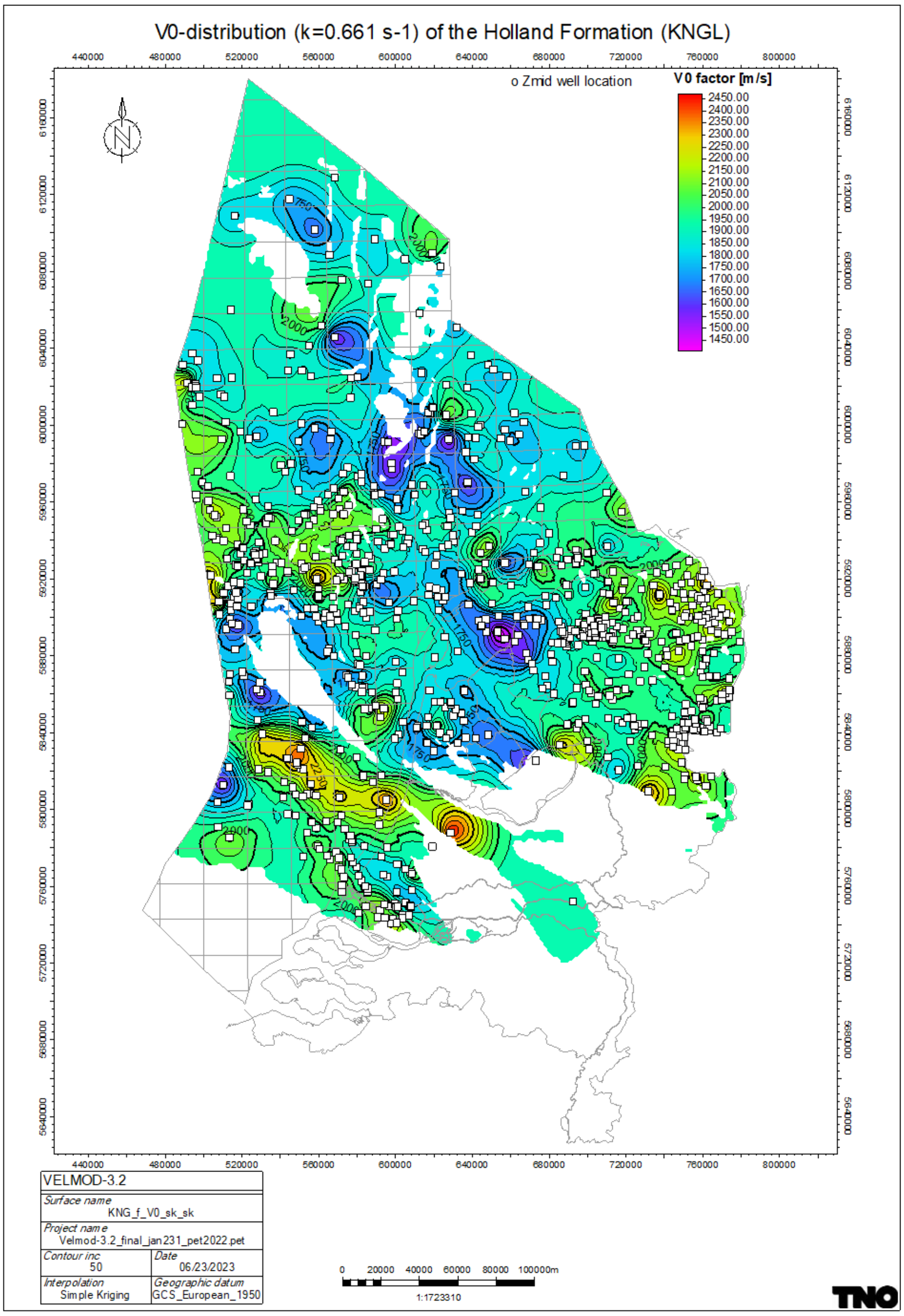

Figure 4.6 V_0 distribution of the Holland Formation.

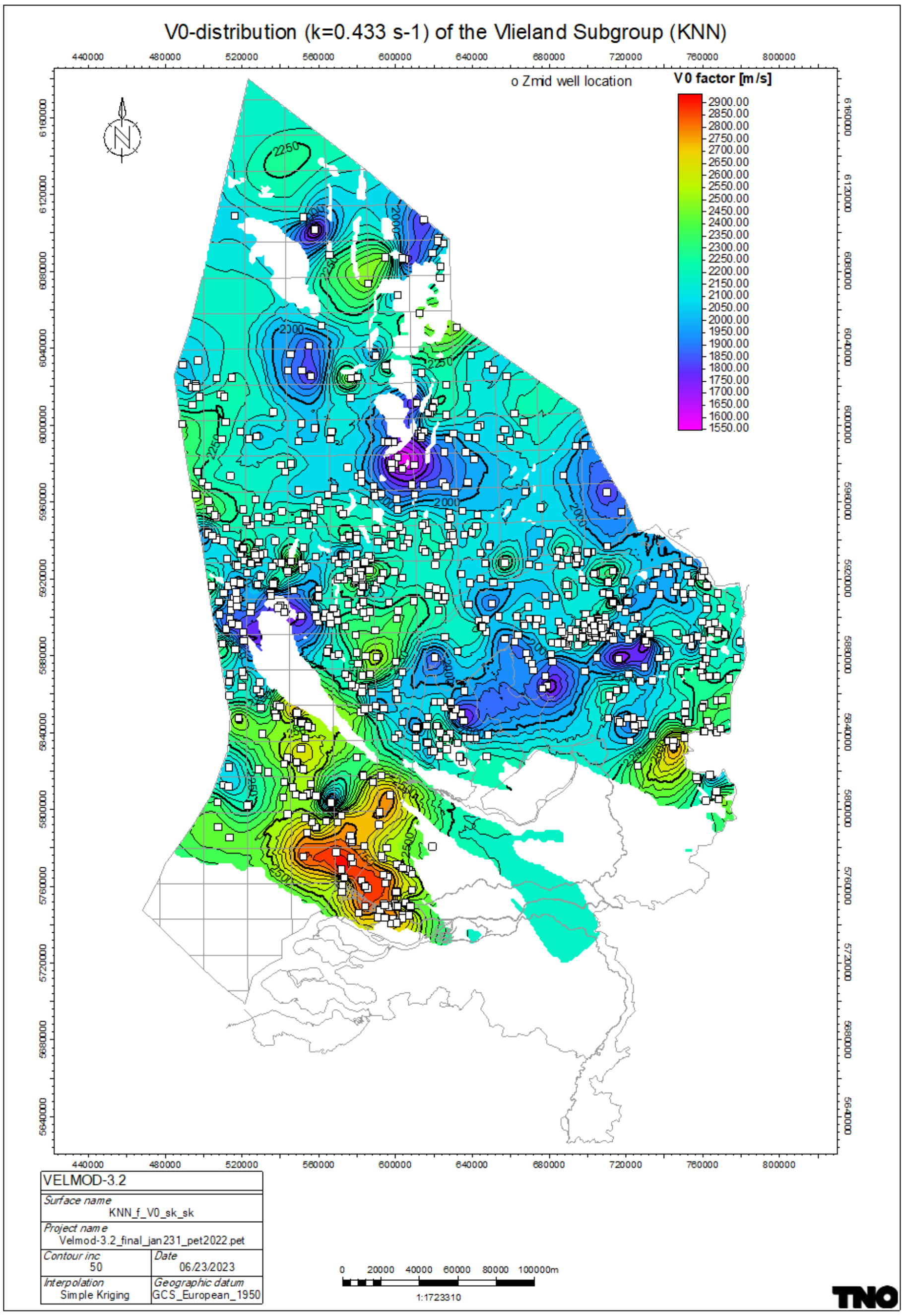

Figure 4.7 V_0 distribution of the Vlieland Subgroup.

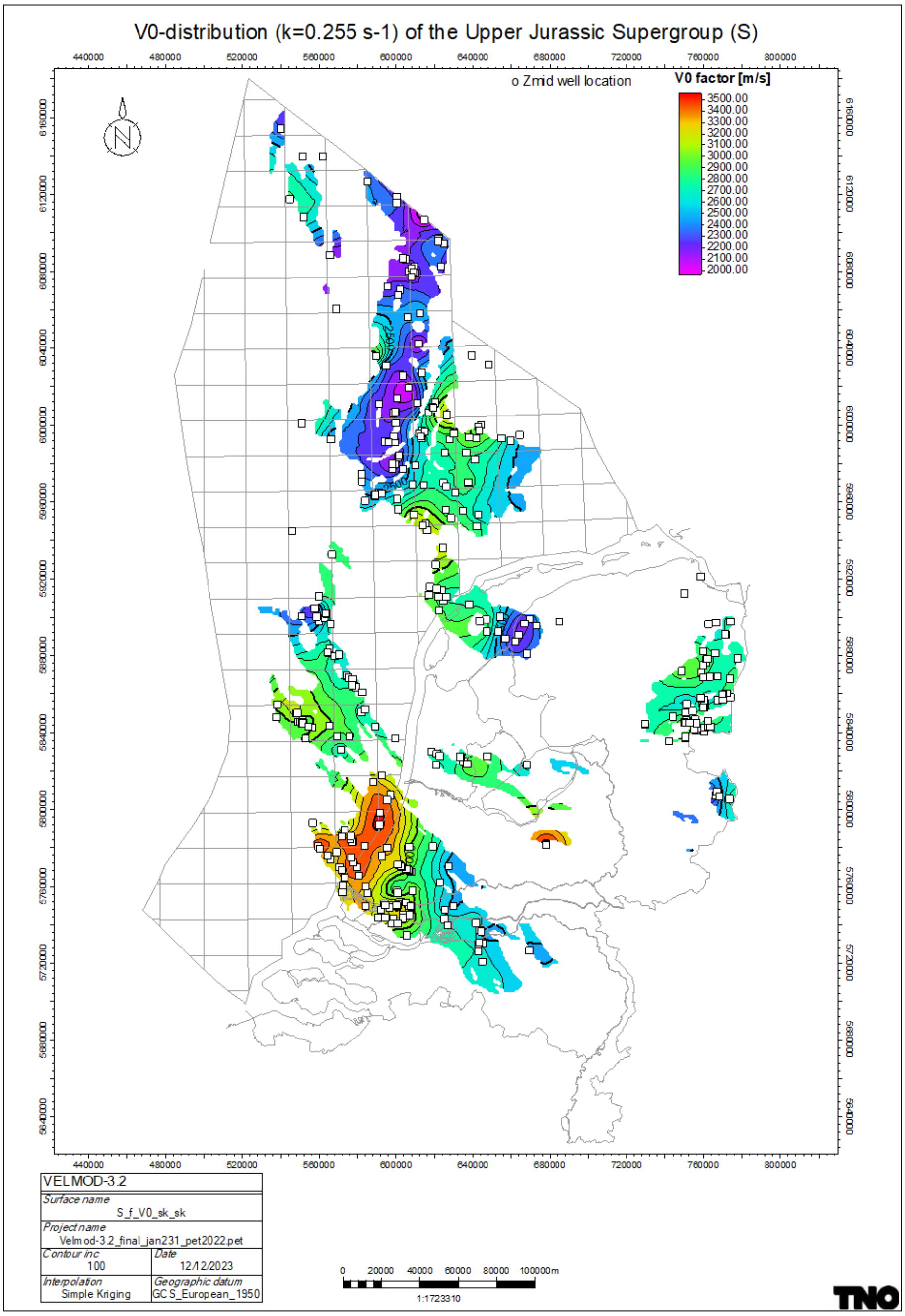

Figure 4.8 V_0 distribution of the Upper-Jurassic Supergroup.

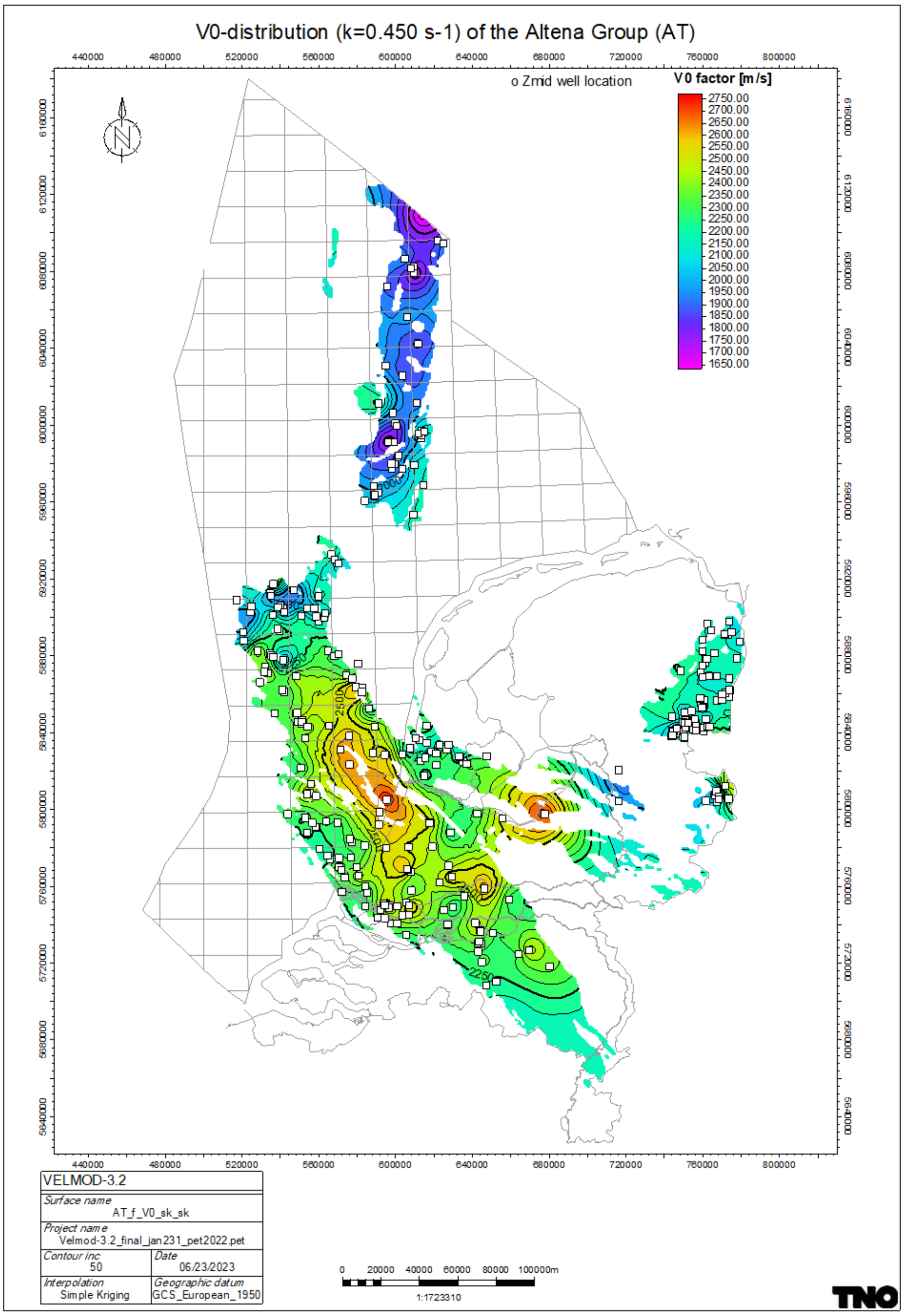

Figure 4.9 V_0 distribution of the Altena Group.

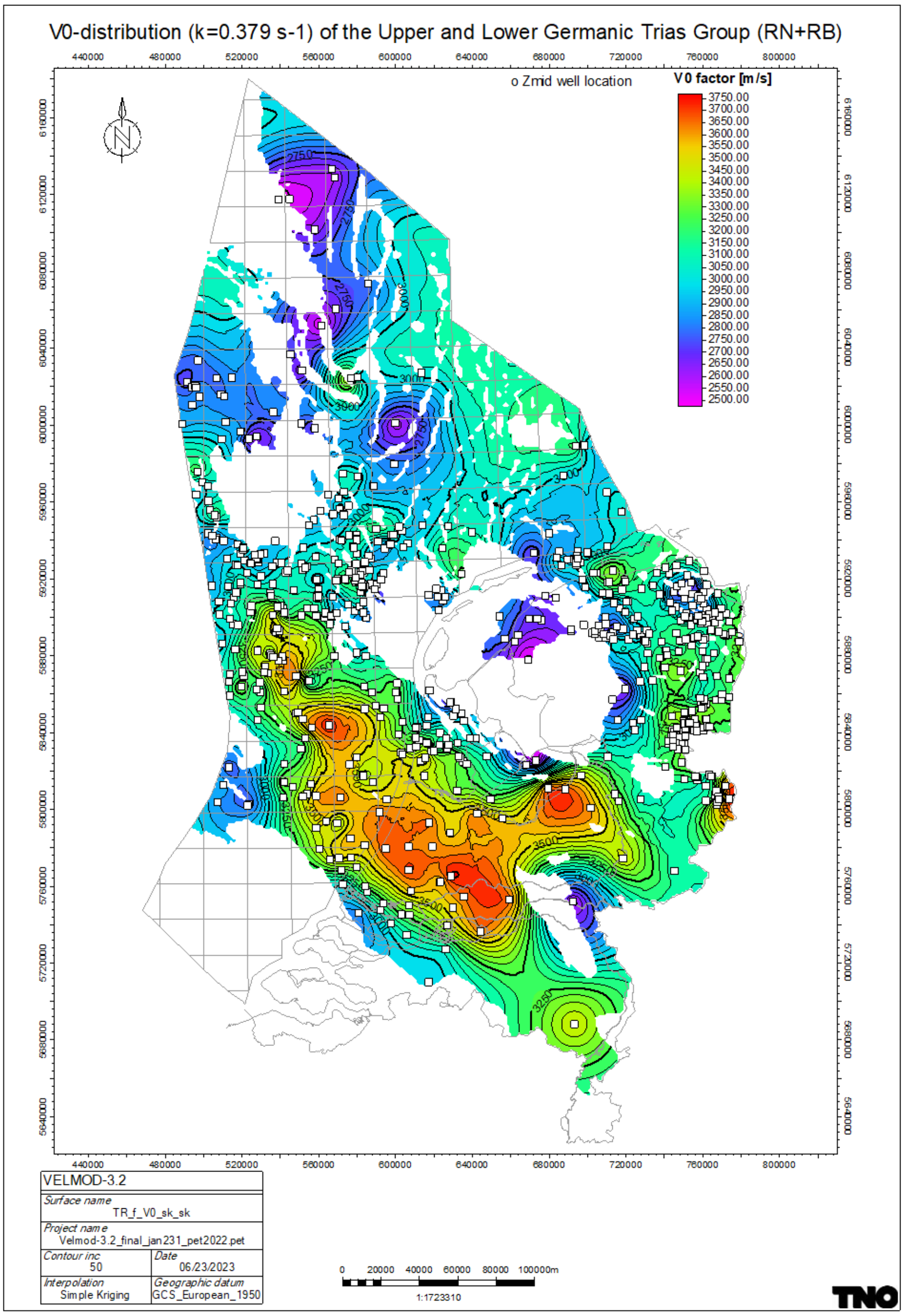

Figure 4.10 V_0 distribution of the Upper and Lower Germanic Trias groups.

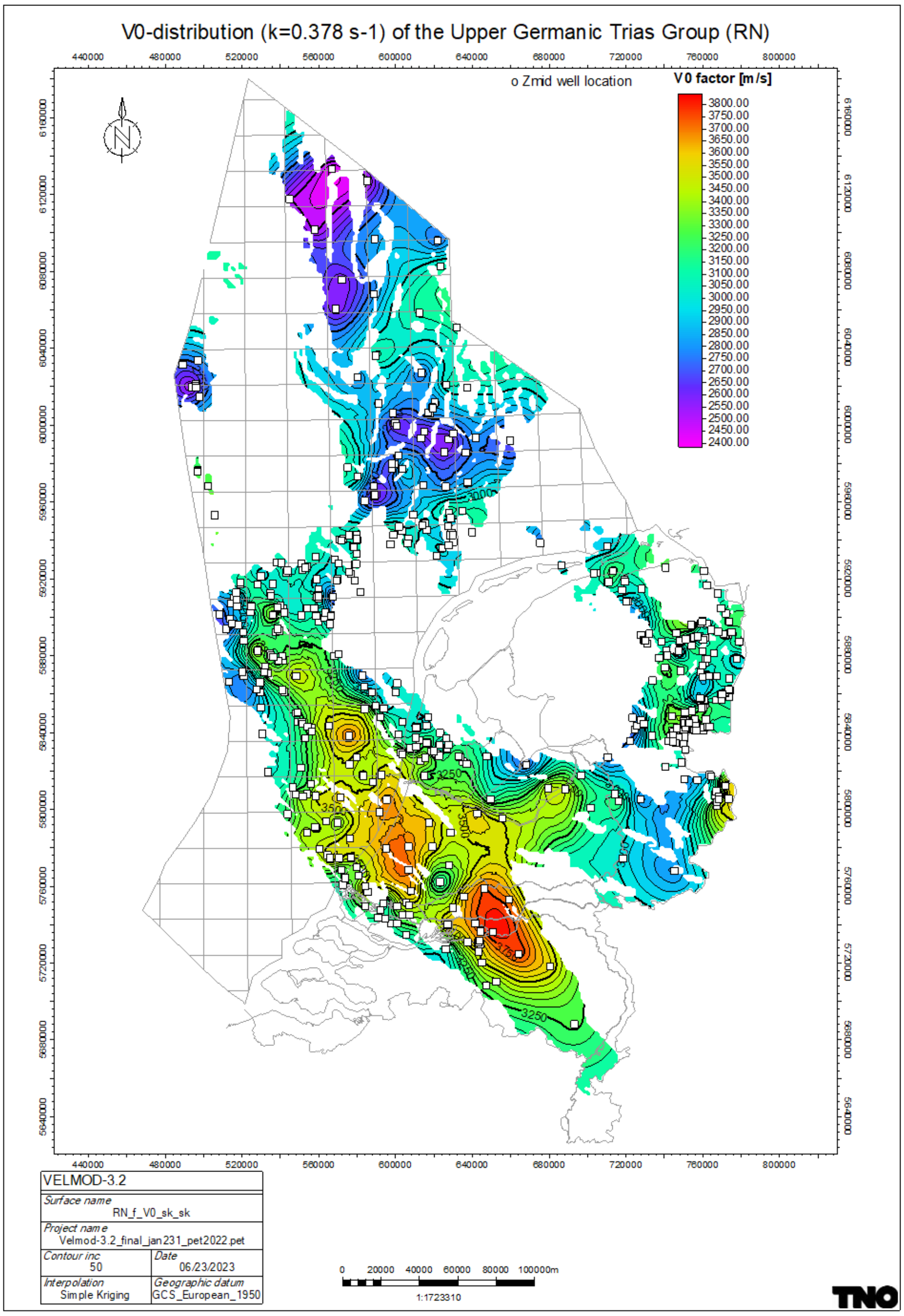

Figure 4.11 V_0 distribution of the Upper Germanic Trias Group.

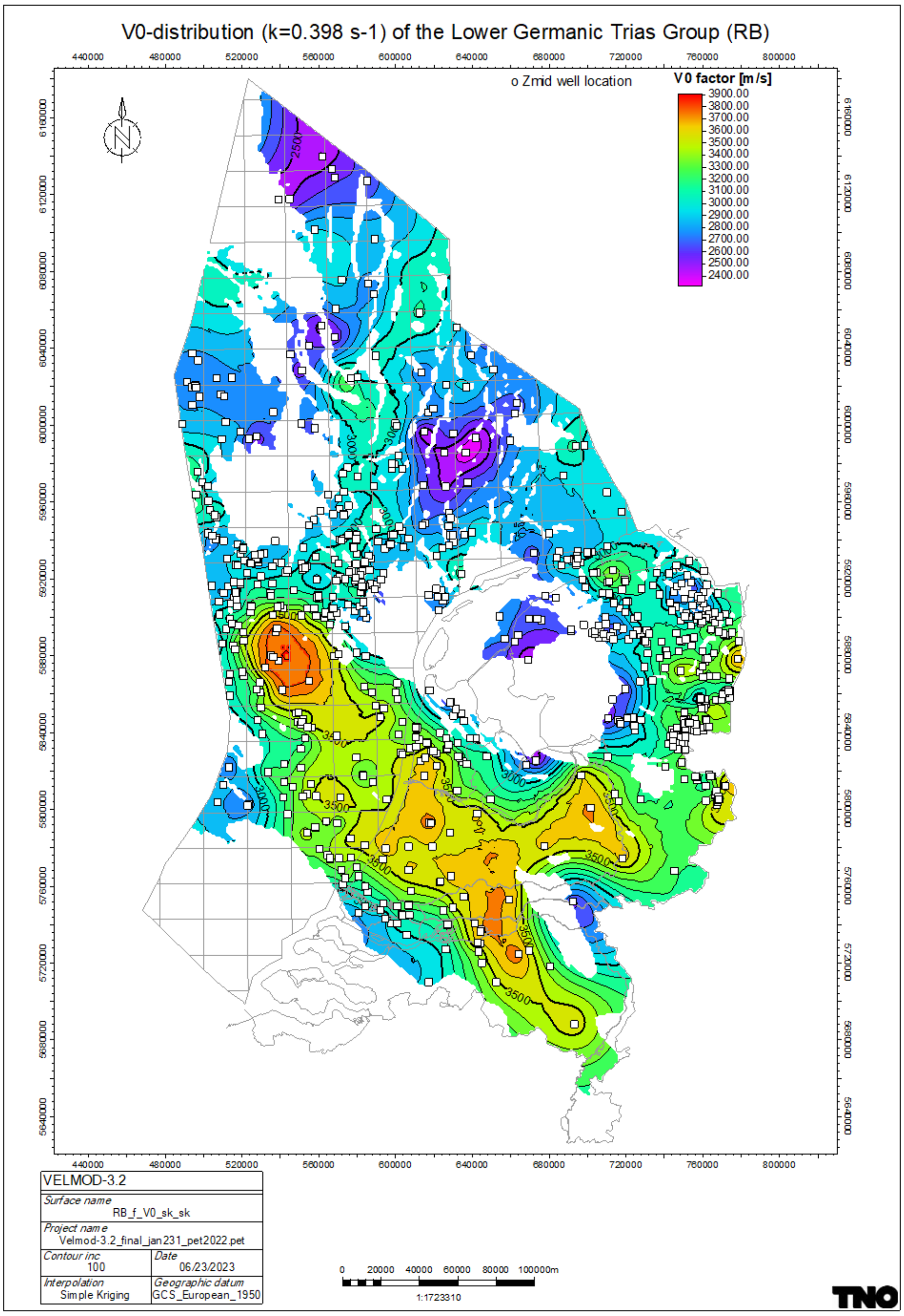

Figure 4.12 V_0 distribution of the Lower Germanic Trias Group.

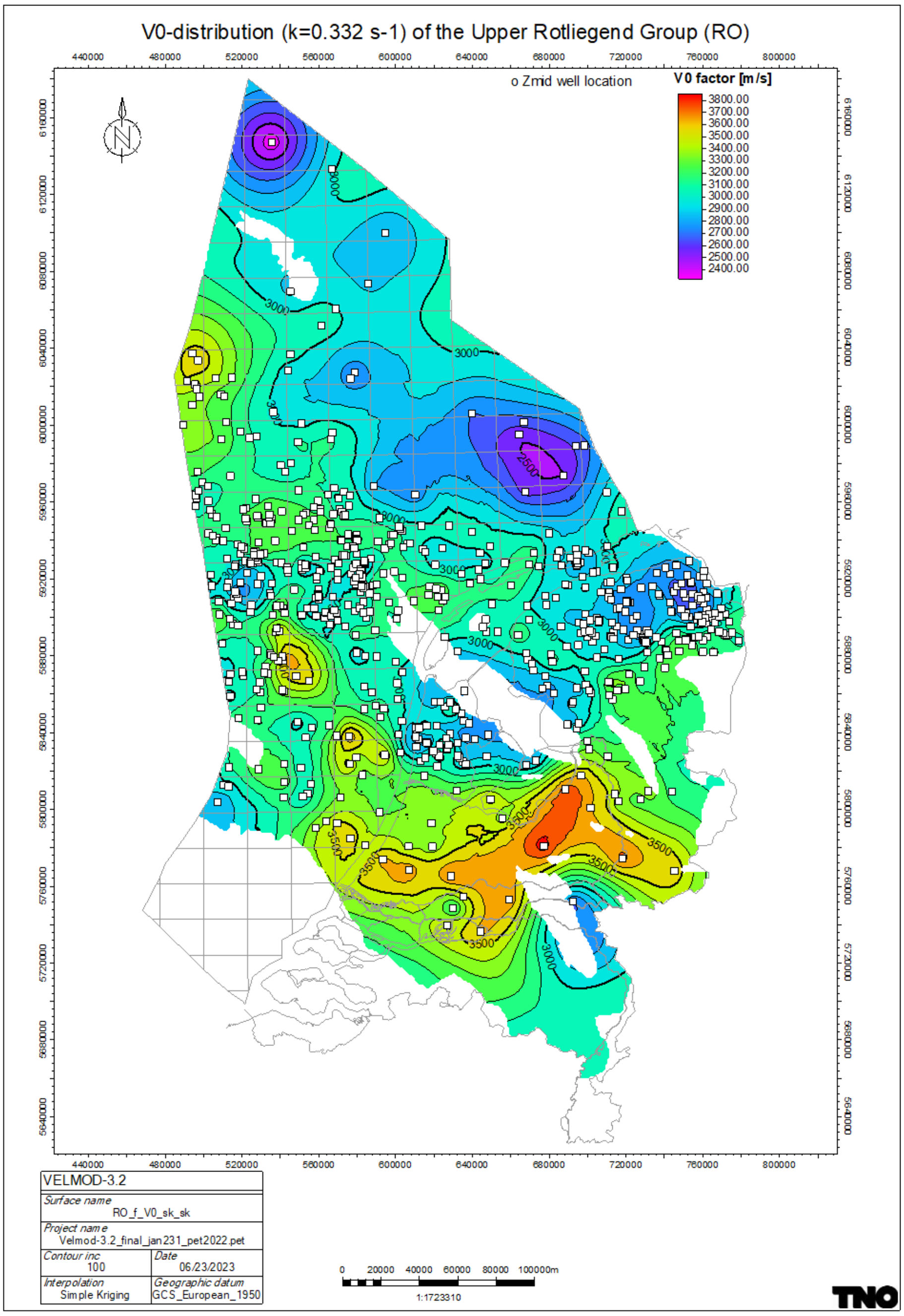

Figure 4.13 V_0 distribution of the Upper Rotliegend Group.

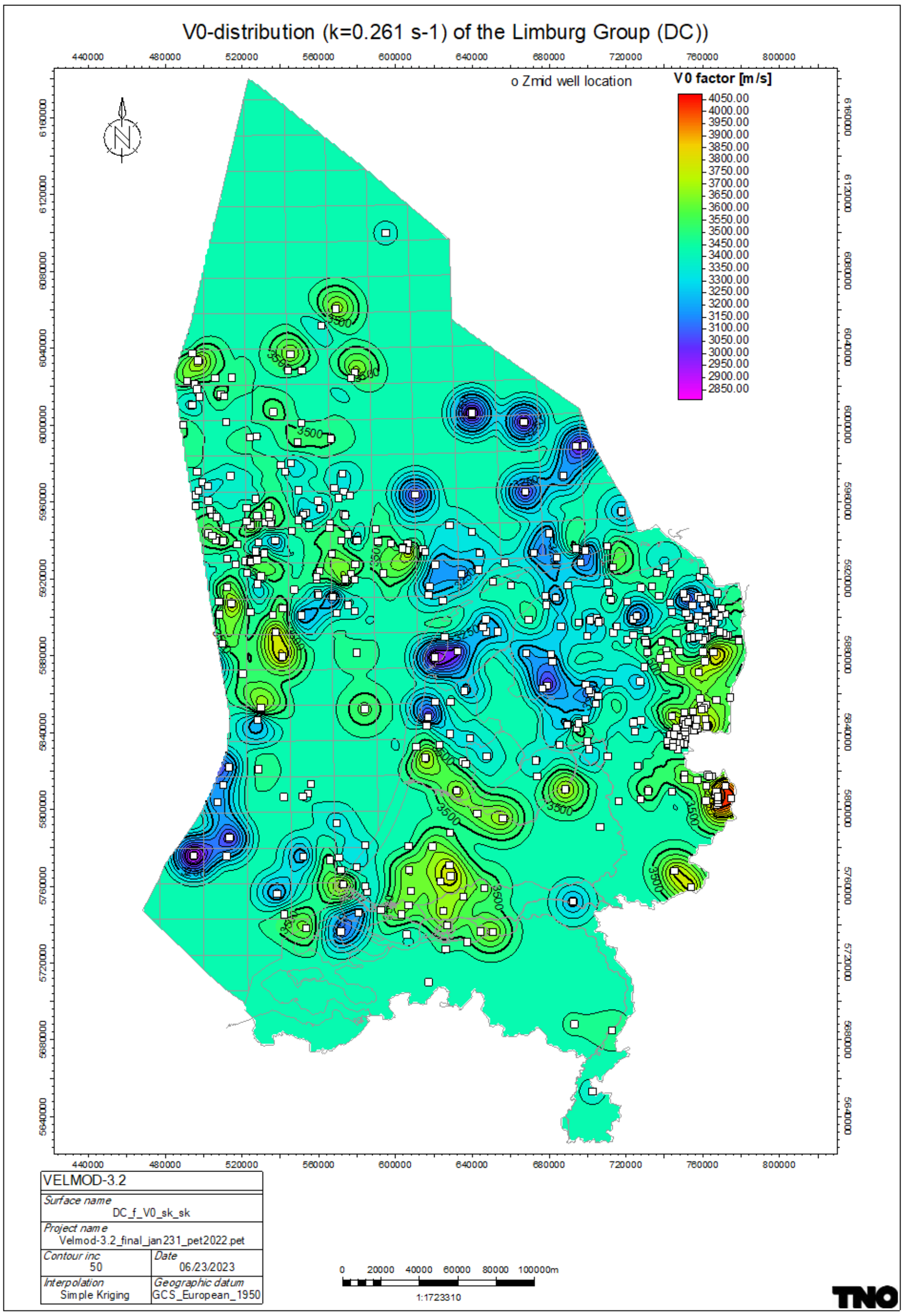

Figure 4.14 V_0 distribution of the Limburg Group.

5 Comparison of VELMOD-3.2 against VELMOD-3.1

This section covers the comparison of VELMOD-3.2 results against VELMOD-3.1 on several data characteristics.

Figure 5.1 shows a comparison of the number of boreholes used per stratigraphic layer for the two models. This highlights an overall decrease in number of used borehole data in VELMOD-3.2 with respect to VELMOD-3.1. This is due to stricter selection criteria used in VELMOD-3.2 resulting in exclusion of more datapoints. This especially affects the shallowest and deepest layers, where sonic data not fully covering the layer was rejected.

The degree of correlation between scatter points from the V_{int}-Z_{mid} analysis (see plots in Figure 3.3- Figure 3.16) was expressed with the correlation coefficient. Figure 5.1 shows a clear overall increase of the correlation coefficient for VELMOD-3.2, indicating the pairs of mid depth and interval velocity are more strongly correlated for VELMOD-3.2. Similarly, the global k-value, which is the slope of the scatter plots from Figure 3.3- Figure 3.16 (also see equation 1), shows an increase for most of the stratigraphic layers for VELMOD-3.2. Increased k-values point at a stronger compactional effect of the overburden on the interval velocity with increasing depth. The normalized velocity (V_0) remains largely unchanged for VELMOD-3.2 as shown in Figure 5.3. Note that changes in k-value and V_0 -values between VELMOD-3.2 andVELMOD-3.1 are not indicative of model improvement or model deterioration.

Although it was beyond the scope of this project to make an extensive comparison of the grids of V_0 and V_{int} between VELMOD3.1 and VELMOD-3.2, overall we did observe a reduction of anomalous outliers in VELMOD-3.2 compared to VELMOD-3.1. This is also visible by less extreme colorbar ranges of V_0 and V_{int} maps in VELMOD-3.2 (this report) compared to VELMOD-3.1 (Pluymaekers et al., 2017).

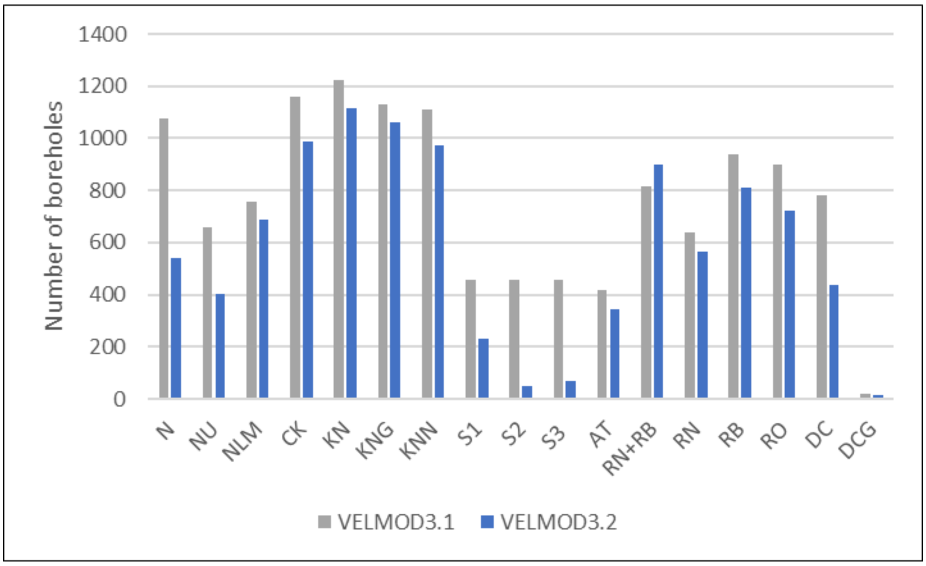

Figure 5.1 Comparison of number of boreholes used per stratigraphic layer for velocity analysis in VELMOD-3.1 (grey) and VELMOD-3.2 (blue).

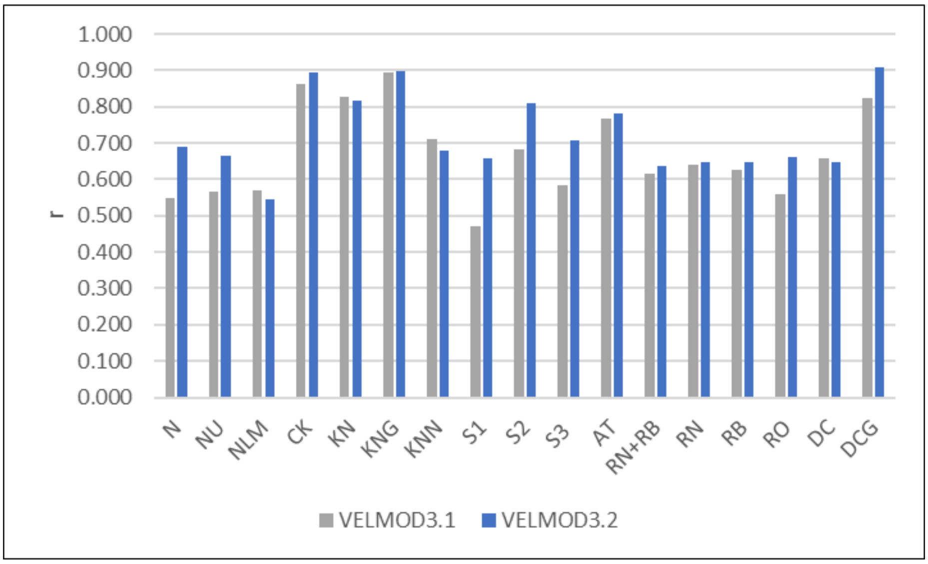

Figure 5.1 Correlation coefficient (r) of the V_{int}-Z_{mid} regression analysis per stratigraphic layer for VELMOD-3.1 and VELMOD-3.2.

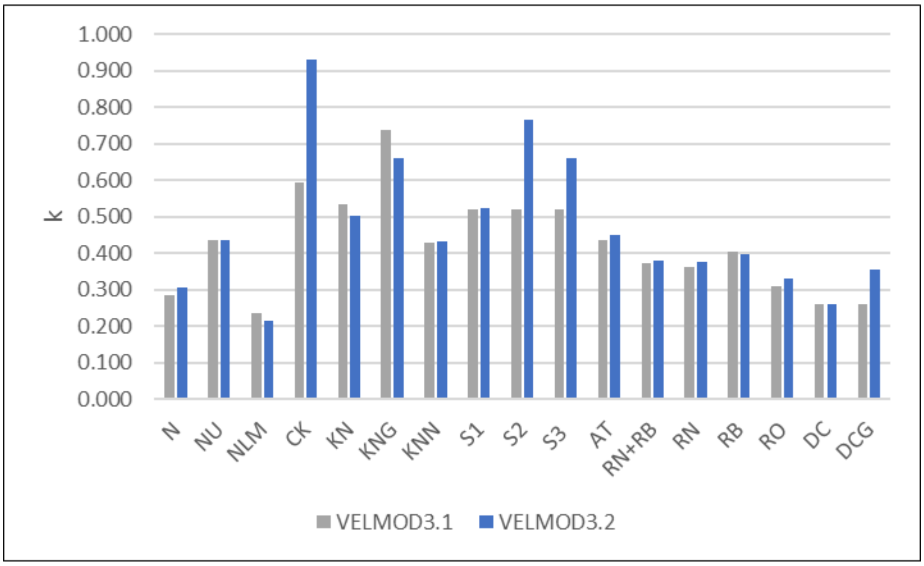

Figure 5.2 Comparison of k global per stratigraphic layer as determined in VELMOD-3.1 (grey) and VELMOD-3.2 (blue).

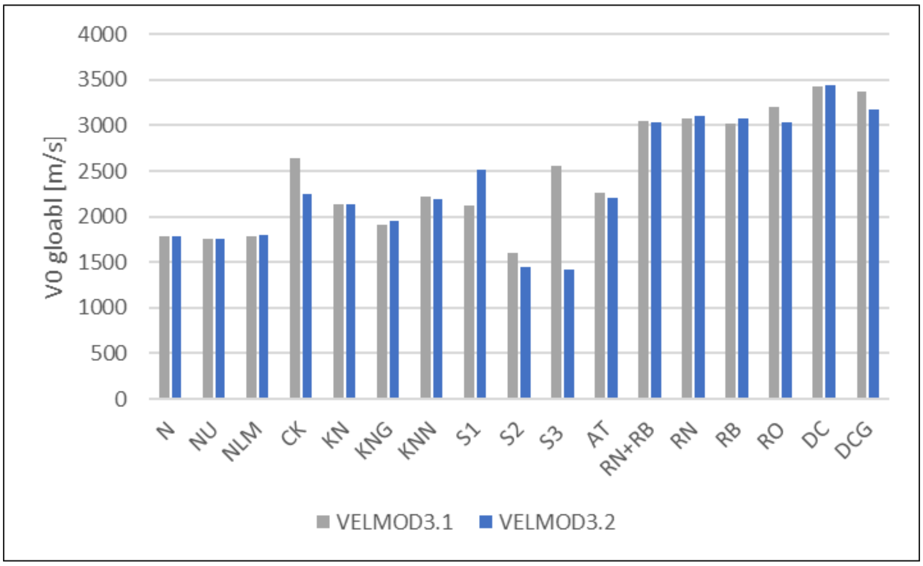

Figure 5.3 Global V_0 per stratigraphic layer as determined in VELMOD-3.1 (grey) and VELMOD-3.2 (blue).

6 Discussion and recommendations

The focus of VELMOD-3.2 was to improve the data selection criteria and to make necessary corrections in the semi-automated workflow as contained in the VELMOD-3.1 workflow. This resulted in a smaller, yet in our opinion -a more trustworthy number of borehole datasets used for the regression analysis from which the normalized velocity and k were calculated. The overall increase in correlation coefficient values found from the regression analysis gives more confidence in the reliability of the data selected and used in VELMOD-3.2 compared to VELMOD-3.1.

Except for the Upper-Jurassic Supergroup, we did not further assess the effect of differentiation into structural elements on the velocity distribution of stratigraphic layers. Only one single k and V_0 was derived for the complete regional dataset of the different lithostratigraphic intervals. For the Upper-Jurassic Supergroup three clustered basins were analysed. The three clusters have a much higher k-value (range k~0.59-0.77) compared to the k value of the Upper-Jurassic Supergroup as a whole (k=0.26). In addition, for example for the Chalk Group (Figure 3.5), a bimodal distribution of V_{int} could be clearly seen, as observed by Pluymaekers et al. (2017). More extensive velocity analysis based on the differentiation of structural elements has been done by Pluymaekers et al. (2017) and Doornenbal et al. (2021). Doornenbal et al. (2021) further addressed the use of regionalized k-values for the Northern offshore and found that this can cause significant distortions in the time-depth process, especially along the boundaries of separate structural elements, and conclude that the success of this approach depends on the structural setting and areal extent of the model. Analysis of the Upper-Jurassic Supergroup shows that each of the clustered basins have similar regionalized k values. However, deriving a global k-value for the complete regional dataset leads to a lower k value, and so underestimation of velocity increase with depth.

The V_0-k model is the preferred model for TNO for regional time-depth conversion. Besides the V_0-k model, a V_{int} model was constructed and described in this report, which was based on simple kriging. The V_{int} model (especially the V_{int} *simple kriging*) is a pure representation of the interval velocities measured in the boreholes and is not subject to model assumptions made in the V_0-k model. It therefore can help a geologist with the validation of a velocity model and resulting time-depth conversion.

The primary goal of VELMOD-3.2 was the construction of a regional velocity model for the use of time-depth conversion of regional seismic interpreted horizons. However, the V_0-distributions for several layers can be interpreted in geological terms of for example: overpressured pore fluids, burial anomalies, or variations in lithology/reservoir properties. These effects can be causing anomalous velocity values on a more local scale, which can better be interpreted from the resulting velocity maps in combination with a structural element map and facie map. The spatial interpolation of the velocity data can be improved by incorporating regional knowledge on overpressured areas and areas subject to phases with major uplift (Pluymaekers et al., 2017).

We conducted manual quality control of the resulting velocity maps to a certain extent. We inspected the more obvious excessive anomalous velocity values, judged their trustworthiness, and decided to accept or reject these datapoints in the regression analysis. However, it was beyond the scope and budget of this project to adopt a very thorough manual QC approach and the presence of some remaining erroneous datapoints cannot be ruled out. Therefore, the user is advised to make his/her own quality checks when using the VELMOD-3.2 results.

A future improvement for VELMOD is the extra option to include additional velocity data. This can concern either new velocity data not contained in VELMOD yet, or existing velocity data not meeting the selection criteria of VELMOD, but of added value due to data scarcity. For instance, on the Belgian side of North Brabant, Belgium velocity data of KB-198 data at Molenbeersel did not pass the data selection criteria of VELMOD-3.2 due to stricter selection criteria, although it did pass the data selection criteria in VELMOD-3.1. This dataset could still be of added value though to actually use in VELMOD, because there is very limited velocity data present in this border region.

Finally, since VELMOD-4 (Doornenbal et al., 2020) relies on both velocity well-data from VELMOD-3.1 and post-stack seismic data from 3D cubes, we recommend a future update of VELMOD-4 based on the velocity well-data used in VELMOD-3.2.

7 References

Doornenbal, J.C., Middelburg, H., de Haan, H., and Botz M., 2020, VELMOD-4, TNO 2020 R10558

Doornenbal, J.C., den Dulk, M., Thöle, H., Jähne-Klingberg, F., Britze, P. & Jakobsen, F. (2021): Deliverable 3.7 – A harmonized cross-border velocity model. GEOERA 3DGEO-EU; 3D Geomodeling for Europe; project number GeoE.171.005., Report, 33 p.

Japsen, P., 1993. Influence of lithology and Neogene uplift on seismic velocities in Denmark: implications for depth conversion of maps. American Association of Petroleum Geologists Bulletin 77, No.2: 194-211.

Kombrink, H., Doornenbal, J.C., Duin, E.J.T., den Dulk, M., van Gessel, S.F., ten Veen, J.H. & Witmans, N., 2012. New insights into the geological structure of the Netherlands; results of a detailed mapping project. Netherlands Journal of Geosciences 91-4, 419 - 446.

Pluymaekers, M.P.D., Doornenbal, J.C., Middelburg, H., 2017, VELMOD-3.1, TNO 2017 R11014 with erratum page 67

ten Veen J.H., van Gessel S.F., den Dulk M., 2012, Thin- and thick-skinned salt tectonics in the Netherlands; a quantitative approach. Netherlands Journal of Geosciences - Geologie en Mijnbouw. 91(4):447-464. doi:10.1017/S0016774600000330

Van Adrichem Boogaert, H.A. & Kouwe, W.F.P., 1993-1997 (eds). Stratigraphic nomenclature of the Netherlands, revision and update by RGD and NOGEPA, Mededelingen Rijks Geologische Dienst, nr. 50.

8 Signature

Naam en ondertekening 2^{e} lezer

ValidSigned by Stefan Peeters
on 2024-06-04 10:24:15

MSc. S. Peeters

Ondertekening

ValidSigned by Bob Paap
on 2024-06-04 10:48:02

MSc. B. Paap
Auteur

Autorisatie vrijgave

ValidSigned by Denise Maljers
on 2024-06-04 10:39:38

Drs. D. Maljers
Research Manager

A Velocity model well results

See results file: *VELMOD3_2_all_welldata.xlsx*
The headers of the column names in this Excel-file are described in Table 8.1

Table 8.1 Column description of VELMOD3_2_all_welldata.xlsx

Column name	Description
short_nm	well name
strat_cd	stratigraphic interval
dataset	file name of data
use_status	False = discard by QC
filtered	True = used for regression line
preferred	True = preferred dataset for well/strat combi
xmid	x coord mid depth
ymid	y coord mid depth
zmid	mid depth of strat interval
dz	thickness stat interval
matching_interval	coverage of data compared to strat interval
vint	Interval velocity (dz/dt)
vmean	average velocity (average of velocity values)
vsd	standard deviation of velocity (vmean)
count	nr of datapoints
variation	variance of velocity (vmean)
bin_mode	mode of binned dataset
bin_freq	frequentie od mode bin
bin_size	in m/s
v0global	V0 global
v0local	V0 local
v0local_basefit	V0 local, error at base level was minimized
kglobal	k global
rmslocal	rms error of V0 local fit
dt_well	delta time in well
dt_seis	delta time from seismic interpretation
dz_vint	model residuals Vint model (depth error)
dz_v0k	model residuals V0-k model (depth error)
dz_v0k_basefit	model residuals V0-k basefit model (depth error)
is_calibrated	velocity data starts at z=0
has_truncated_base	missing velocity data in lower part stratigraphic section
has_truncated_top	missing velocity data in upper part stratigraphic section
vel_type	type of data used (sonic/cs/tz)
vel_src	source data type (las curve)
flag	remarks
duplicate	marked as duplicate x,y values

Table 8.2 Description of velocity source data types used

vel_src	vel_type	refers to the type of velocity measurement
dt	son	unspecified sonic log
twt	twt	two way time derived form unspeciefied source (checkshots)
ac	son	acoustic log
son	son	unspecified sonic log
timc	owt	corrected travel time
dtc	son	corrected sonic log
twotim	twt	two way time derived form unspeciefied source
vel	vel	velocity derived form unspeciefied source
owt	owt	one way time derived form unspeciefied source
dtcocal	son	calibrated (compressional) sonic log
dtc_cal	son	calibrated corrected sonic log
dtl	son	long spaced sonic
dtcl	son	unspecified sonic log
dtlf	son	long spaced sonic far
dtln	son	long spaced sonic near
dtco	son	(compressional) sonic log
intt	son	interval transist time
dtc_ed_cal	son	calibrated corrected sonic log, edited
dtc_ed	son	corrected sonic log, edited
dtc_edt_cal_winz	son	calibrated corrected sonic log, edited
dtc_m-s	son	corrected sonic log
dtc_cal_ssl	son	calibrated corrected sonic log
dtin	son	delta t input
dt_cal_winz	son	calibrated sonic log
dtc_edited	son	corrected sonic log, edited
dtc_cal_winz	son	calibrated corrected sonic log
dtc_edt	son	corrected sonic log, edited
dt_mmk	son	unspecified sonic log
dtc cal	son	calibrated corrected sonic log
dtc-cal vel	son	calibrated corrected sonic log

Table 8.3 Description of velocity measurement type

vel_type	refers to unit of velocity measurement
son	sonic log [us/ft]
owt	one way travel time [s, or ms]
twt	two way travel time [s, or ms]
vel	velocity [m/s]

B V_{int}, V_0 & kriging standard deviation grids

The following VELMOD-3.2 products can be found on nlog.nl:

- V_{int} grids and figures
- V_0 grids and figures
- V_0 standard deviation grid and figures

C T/Z pairs

See results file: velmod3_all_tz_basefit.xlsx
The headers of the column names in this Excel-file are described in Table 8.4.

Table 8.4 Description of the column names of velmod3_all_tz_basefit.xlsx

short_nm	well name
strat_base_cd	stratigraphic interval code
x	x coordinate
y	y coordinate
z	depth of base stratigraphic interval
t	time of base stratigraphic interval (OWT)
t_alt	alternative time of base stratigraphic interval (OWT)
remark	remarks
dataset	file name of dataset
preferred	True = preferred dataset for well/stratigraphy combination
calibrated	velocity data starts at z=0